ARMY RESEARCH LABORATORY

Point Picking and Distributing on the Disc and Sphere

by Mary K Arthur

ARL-TR-7333 **July 2015**

NOTICES

Disclaimers

The findings in this report are not to be construed as an official Department of the Army position unless so designated by other authorized documents.

Citation of manufacturer's or trade names does not constitute an official endorsement or approval of the use thereof.

Destroy this report when it is no longer needed. Do not return it to the originator.

Army Research Laboratory
Aberdeen Proving Ground, MD 21005-5066

ARL-TR-7333 **July 2015**

Point Picking and Distributing on the Disc and Sphere

Mary K Arthur
Weapons and Materials Research Directorate, ARL

REPORT DOCUMENTATION PAGE	Form Approved OMB No. 0704-0188

1. REPORT DATE *(DD-MM-YYYY)*	2. REPORT TYPE	3. DATES COVERED (From - To)
July 2015	Final	October 2013–September 2014

4. TITLE AND SUBTITLE
Point Picking and Distributing on the Disc and Sphere

5a. CONTRACT NUMBER

5b. GRANT NUMBER

5c. PROGRAM ELEMENT NUMBER

6. AUTHOR(S)
Mary K Arthur

5d. PROJECT NUMBER
AH80

5e. TASK NUMBER

5f. WORK UNIT NUMBER

7. PERFORMING ORGANIZATION NAME(S) AND ADDRESS(ES)
US Army Research Laboratory
ATTN: RDRL-WML-A
Aberdeen Proving Ground, MD 21005-5066

8. PERFORMING ORGANIZATION REPORT NUMBER
ARL-TR-7333

9. SPONSORING/MONITORING AGENCY NAME(S) AND ADDRESS(ES)

10. SPONSOR/MONITOR'S ACRONYM(S)

11. SPONSOR/MONITOR'S REPORT NUMBER(S)

12. DISTRIBUTION/AVAILABILITY STATEMENT
Approved for public release; distribution is unlimited.

13. SUPPLEMENTARY NOTES

14. ABSTRACT

This report presents a collection of algorithms for picking and distributing points on a disc and sphere. The algorithms presented fall into 2 categories: 1) random point picking and 2) evenly spaced point distributing.

15. SUBJECT TERMS
point picking, evenly spaced points, uniform points, disc, sphere, spiral, analytic, Vogel, sunflower, Archimedes, Fermat, Rakhmanov, Saff, Zhou, Bauer, Thomson, Fejes Tóth, Voronoi, Platonic solid, electrostatic repulsion, geodesic subdivision, discrete extremal energy, stellar attitude determination analysis

16. SECURITY CLASSIFICATION OF:			17. LIMITATION OF ABSTRACT	18. NUMBER OF PAGES	19a. NAME OF RESPONSIBLE PERSON
a. REPORT	b. ABSTRACT	c. THIS PAGE			Mary K Arthur
Unclassified	Unclassified	Unclassified	UU	58	19b. TELEPHONE NUMBER (*Include area code*) 410-278-6110

Standard Form 298 (Rev. 8/98)
Prescribed by ANSI Std. Z39.18

Contents

List of Figures

Acknowledgments

I would like to thank Rew Thompson for his technical review and Langston Willis for his editorial review.

INTENTIONALLY LEFT BLANK.

1. Introduction

Although the analyses performed by the Advanced Lethality and Protection Analysis Branch (ALPAB) of the Weapons and Materials Research Directorate, US Army Research Laboratory, are extremely varied and diverse, some scenarios arise with a not unexpected consistency. It is not uncommon for ALPAB analyses to require a grid scheme or uniform random point picking over a given domain. A few general examples of this are random personnel or vehicle targets spread across an area target, evenly distributed sample points structured to allow for unbiased spatial data collection, and space-filling vehicle or projectile formations (e.g., potential swarming applications).

Point picking and evenly spaced point distributing over a parallelogram or parallelepiped domain are straightforward and intuitive. The most basic example of evenly spaced point distributing over a parallelogram or parallelepiped is the set of vertices of a Cartesian grid. Most scientists, engineers, and laypersons alike are familiar and comfortable with the concept of using a Cartesian grid to evenly partition Euclidean space. However, the process of point picking or distributing over other domains is not always as straightforward. More specifically, point picking and especially evenly spaced point distributing over circular and spherical domains turns out to be a much more difficult problem, and unfortunately, such domains are regularly required or desired.

Point picking on the disc has most recently and regularly been used by ALPAB analysts to calculate the positions of individual personnel and vehicle targets over a circular area battlefield. One specific example of such a target was used in the Modular-Munition, Dual-Warhead Concept Analysis.[1] The battlefield target in this analysis was supposed to loosely represent how an assembly or staging consisting of both personnel and vehicle targets might look. This circular area target was also used in subsequent analyses such as the Modular Lethality Multi-Target Defeat analysis.[2] Evenly spaced point distribution has most recently become a tool in the Modular Lethality effort as well and has been applied to the positioning of a set of individual projectiles that are assumed to be able to work in a specific formation to defeat the given target.[3] Evenly spaced point distribution over a disc or even on or within a sphere will most likely play a role in many “swarming” type concept analyses in the future.

The ALPAB project that finally spurred the collection of point picking and distributing algorithms and the writing of this report was Adaptive Protection: the Dynamic Threat Map (DTM). The objective of the DTM was to develop a set of algorithms for predicting the potential for threat (i.e., future threats) around a vehicle’s current location based off of both historical and real time situational data. Part of the algorithm development necessitated the fast computation of an arbitrary number of evenly spaced data collection rays emanating from the center of mass of the vehicle. This is exactly the problem of even point distribution on the surface of the sphere (hemisphere in this particular case).

These are just a few examples of the ALPAB projects over the past 2 years that have implemented algorithms for picking and distributing points on a disc or sphere. In actuality, the author estimates that she is asked about point picking and distributing algorithms at least once every other month. It is with this in mind that in this report we present a collection of algorithms for picking and distributing points on a disc and sphere. In computer simulation, the need to arrange points on a disc or on or within a sphere commonly falls into 2 categories: 1) random point picking and 2) evenly spaced point distributing.

Random point picking, or just point picking, is defined in this report as the process of picking random points within the region of interest such that the density of points within arbitrary neighborhoods is expected to be uniform over the entire region as the number of points, *n*, goes to infinity. Random point picking is very useful when an unstructured (i.e., random) point distribution is desired. However, for small values of *n*, random point picking does not guarantee uniform spatial distribution of points over the region.

Evenly spaced point distributing is defined in this report as the process of distributing *n* points over the surface of the disc or sphere so as to produce the most evenly spaced distribution of points possible. To consistently produce uniform and evenly spaced distributions of points when *n* is small, evenly spaced point distributing techniques often produce structured, grid-like point patterns.

This report does not attempt to document an exhaustive collection of point picking and distributing algorithms but instead focuses on the small handful that the author has found to be most useful for her purposes. All calculations are presented for a disc or sphere centered at the origin.

2. Point Picking on (and around) the Disc

2.1 Elimination Method

If runtime is not an issue, an easy method for point picking on a disc of radius *r* is the elimination method. In the elimination method, the x- and y-coordinates of each point are each drawn from a uniform $[-r, r]$ distribution, (i.e., from the smallest square containing the disc). Each point is then either accepted or rejected depending on whether or not it lies within the disc (Fig. 1). This method is simple to implement, but as the disc only occupies approximately 79% of the area within this square domain, approximately 21% of the points picked will be rejected (Fig. 1). For this reason, it is often desired to implement a direct method that does not rely on picking and eliminating points.

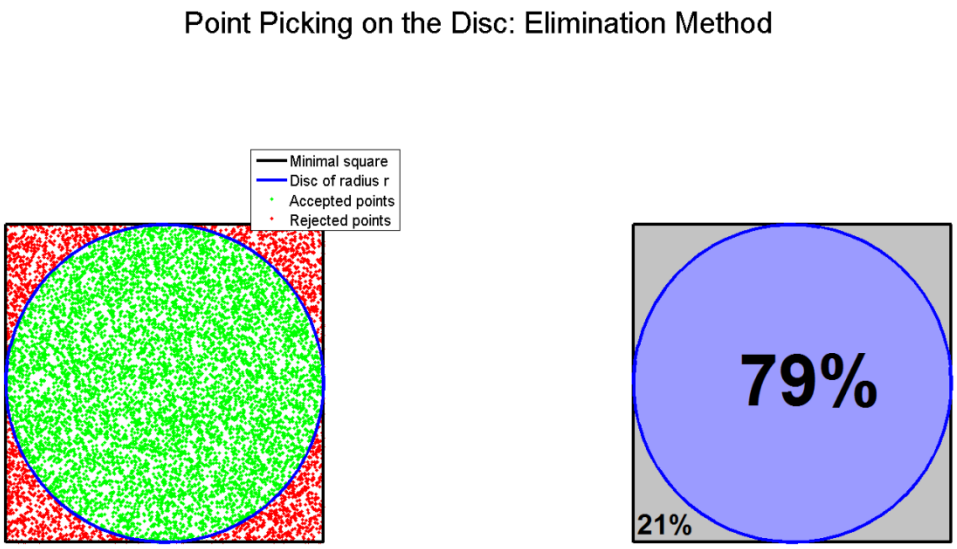

Fig. 1 Elimination method for point picking on the disc. Points are generated over the smallest square region containing the disc and then are rejected if they do not lie within the disc. Only about 79% of points will be accepted with approximately 21% being rejected.

2.2 Direct Method: The Most Common Mistake

When point picking over a rectangular domain $[a, b] \times [c, d] \subset \mathbb{R}^2$, most people will quickly realize that the most straightforward technique is to draw an x-coordinate from a uniform $[a, b]$ distribution, and a y-coordinate from a uniform $[c, d]$ distribution. The resulting points will exhibit a uniform spatial distribution over the domain (Fig. 2).

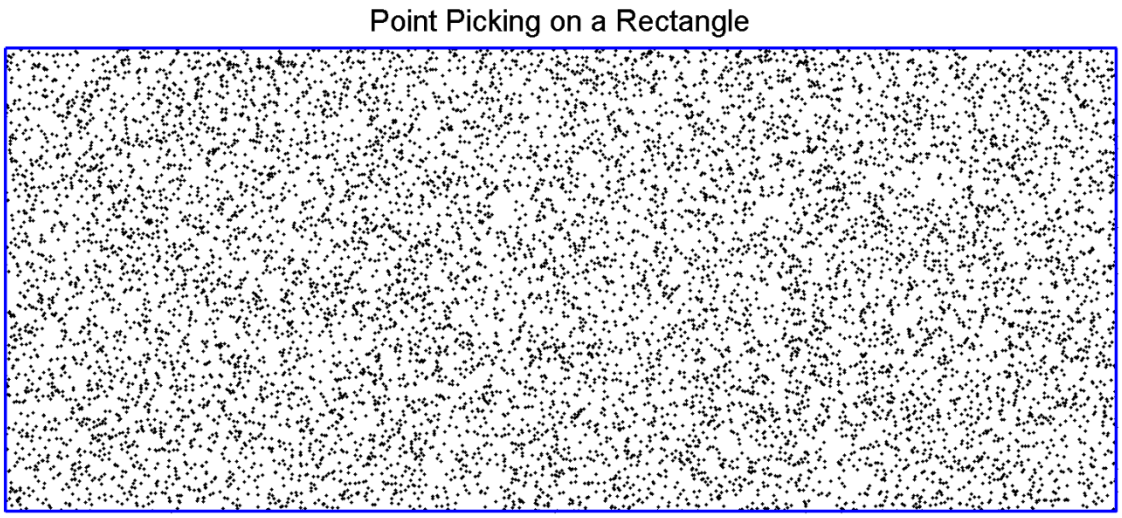

Fig. 2 Point picking on a rectangle; x- and y-coordinates are drawn independently from uniform distributions over their respective domains and yield a uniform spatial distribution over the rectangle

The logical extension of this technique to point picking over a circular domain

$$S^1 := \{(x, y) \in \mathbb{R}^2 \mid x^2 + y^2 \leq r^2\} \tag{1}$$

is to switch to polar coordinates over the domain $[\rho, \theta] \subseteq [0, r] \times [0,2\pi]$. We can then draw ρ from a uniform $[0, r]$ distribution, and θ from a uniform $[0,2\pi]$ distribution, and use the standard polar to Cartesian transformations

$$x = \rho \cos \theta \tag{2}$$

$$y = \rho \sin \theta \tag{3}$$

to get back to the desired Cartesian coordinates. Although the resulting points will have ρ- and θ-coordinates that are independently uniformly distributed, it quickly becomes apparently that the points themselves are “clumped” near the origin and far from uniformly distributed over the disc (Fig. 3).

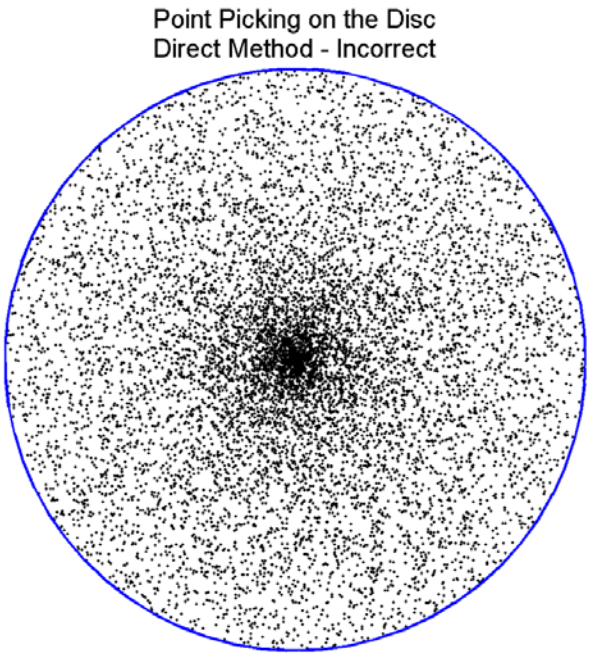

Fig. 3 Point picking on the disc; drawing both ρ- and θ-coordinates from independent, uniform distributions over their respective domains yields a point distribution that is clumped around the center of the disc

There is a simple explanation for this outcome. First, recall that the area of the sector subtended by a central angle, φ, of a circle of radius r (Fig. 4) is given by the equation

$$A = \frac{1}{2} r^2 \, \varphi. \tag{4}$$

Therefore, the area of a polar rectangle about a point, p, as shown in Fig. 5 can be expressed as

$$dA = A_2 - A_1 = \frac{1}{2}\rho_2^2 \, d\theta - \frac{1}{2}\rho_1^2 \, d\theta = \frac{1}{2}(\rho_2^2 - \rho_1^2) \, d\theta. \tag{5}$$

This can be expanded to

$$dA = \frac{1}{2}(\rho_2 + \rho_1)(\rho_2 - \rho_1) \, d\theta = \frac{1}{2}(\rho_2 + \rho_1) \, d\rho \, d\theta = \rho \, d\rho \, d\theta, \tag{6}$$

where

$$\rho = \frac{1}{2}(\rho_2 + \rho_1). \tag{7}$$

Equation 6 is commonly referred to as the area element and should be familiar to anyone who has evaluated a double integral in polar coordinates.

So when point picking on the disc, although the density of ρ-coordinates over any change in ρ (i.e., over any $d\rho$) and the density of θ-coordinates over any change in θ (i.e., over any $d\theta$) remain the same, the area of the resulting polar rectangle (i.e., the area element) is given by

$$dA = \rho \, d\rho \, d\theta. \tag{8}$$

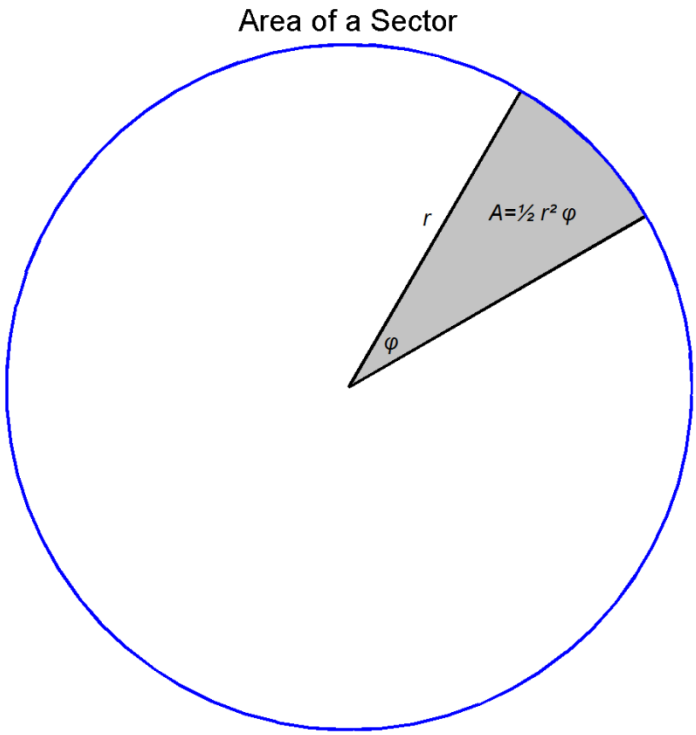

Fig. 4 Area of a sector of a circle

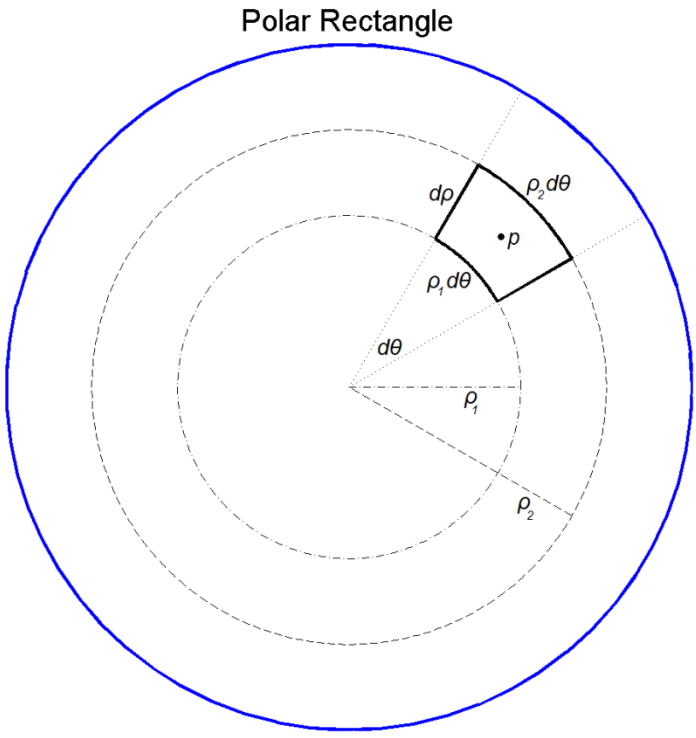

Fig. 5 Example of a polar rectangle

This means that for any 2 polar rectangles with equal $d\rho$s and $d\theta$s, the number of points within the polar rectangles will be equal; however, the area, and therefore density of points within each polar rectangle will directly depend on the ρ-coordinate of that particular polar rectangle (Fig. 6).

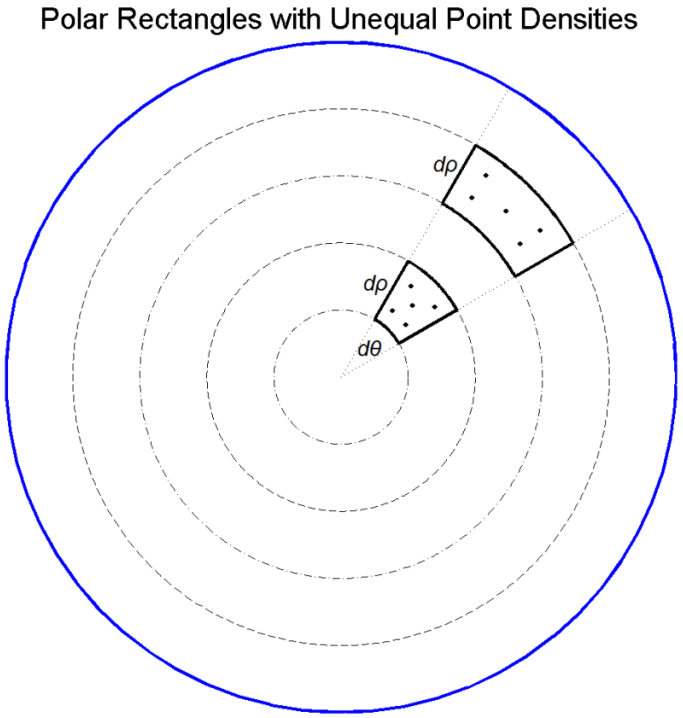

Fig. 6 Two area elements with equal radial lengths ($d\rho$) and angular components ($d\theta$) but different areas

2.3 Direct Method: A Simple Transform

Luckily, there is a rather intuitive solution to the "clumping problem". We need only to find the appropriate coordinate transform to remove the radial coordinate dependence from the area of the polar rectangle. To be exact, we are looking for a coordinate transform of the form

$$u = f(\rho), \quad f: [0, r] \to [a, b], \; f \in C^1 \,, \tag{9}$$

such that

$$du = \rho \, d\rho. \tag{10}$$

Then the area element in Eq. 8 would become

$$dA = \rho \, d\rho \, d\theta = du \, d\theta. \tag{11}$$

Integrating Eq. 11 yields the desired transformation

$$u = \tfrac{1}{2}\rho^2, \quad u: [0, r] \to \left[0, \tfrac{1}{2}r^2\right]. \tag{12}$$

For convenience, we multiply by 2 and adjust the interval to yield

$$u = \rho^2, \quad u: [0, r] \to [0, r^2]. \tag{13}$$

Finally, to make use of the transform, we solve for ρ to yield

$$\rho = \sqrt{u}, \quad \rho: [0, r^2] \to [0, r]. \tag{14}$$

With this coordinate transform, the direct method for point picking over a disc of radius r reduces to drawing u from a uniform $[0, r^2]$ distribution, θ from a uniform $[0,2\pi]$ distribution, and applying the transformations

$$x = \sqrt{u}\cos\theta \tag{15}$$

and

$$y = \sqrt{u}\sin\theta. \tag{16}$$

The resulting points no longer exhibit the clumped distribution near the origin (Fig. 7), and it can be easily verified that the points are now uniformly distributed across the disc (left to the reader).

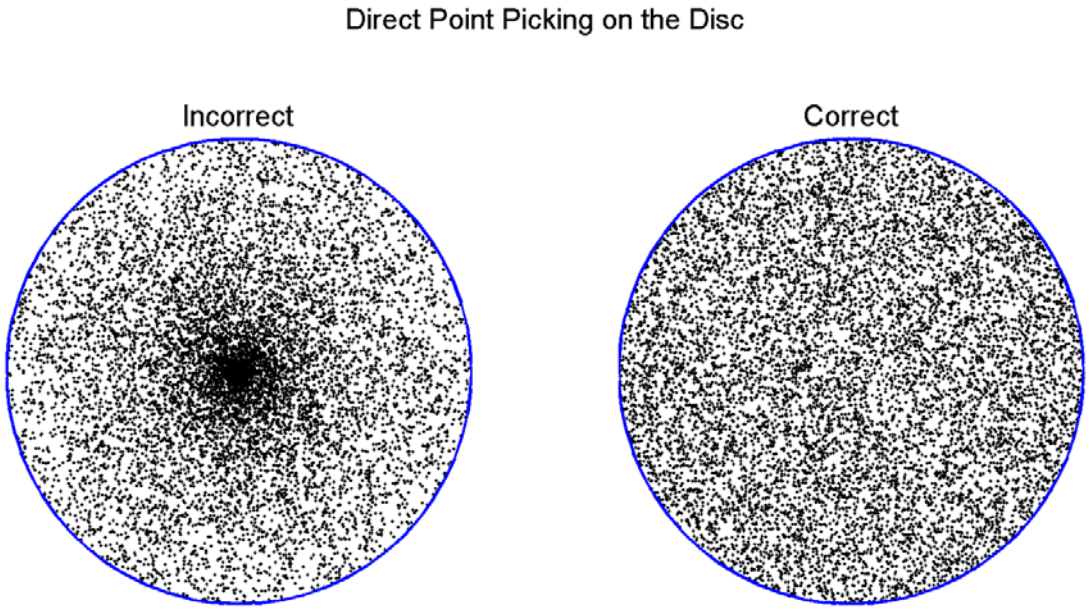

Fig. 7 Side by side comparison of the most common mistake and correct method for directly picking points on the disc

2.4 Points on the Circle

One application, albeit trivial, of the direct point picking method presented in Section 2.3 is picking uniformly distributed points along the boundary of the disc, (i.e., around a circle). The boundary of the disc is the set of points

$$\partial S^1 := \{(x, y) \in \mathbb{R}^2 \mid x^2 + y^2 = r^2\}, \tag{17}$$

which is equivalent to the set

$$\Omega^1 := \{\theta \in [0,2\pi] \mid x = r\cos\theta,\ y = r\sin\theta\}. \tag{18}$$

Therefore, the direct method for point picking around a circle of r reduces to drawing θ from a uniform $[0,2\pi]$ distribution and applying the transformations

$$x = r\cos\theta \tag{19}$$

and

$$y = r\sin\theta. \tag{20}$$

3. Point Picking in (and on) the Sphere

3.1 Elimination Method

If runtime is not an issue, an easy method for point picking within a sphere of radius r is the elimination method. In the elimination method, the x-, y-, and z-coordinates of each point are each drawn from a uniform $[-r, r]$ distribution, i.e., from the smallest cube containing the sphere. Each point is then either accepted or rejected depending on whether or not it lies within the sphere (Fig. 8). This method is simple to implement, but as the sphere only occupies approximately 53% of the volume within this cube domain, approximately 47% of the points picked will be rejected (Fig. 8). For this reason, it is often desired to implement a direct method that does not rely on picking and eliminating points.

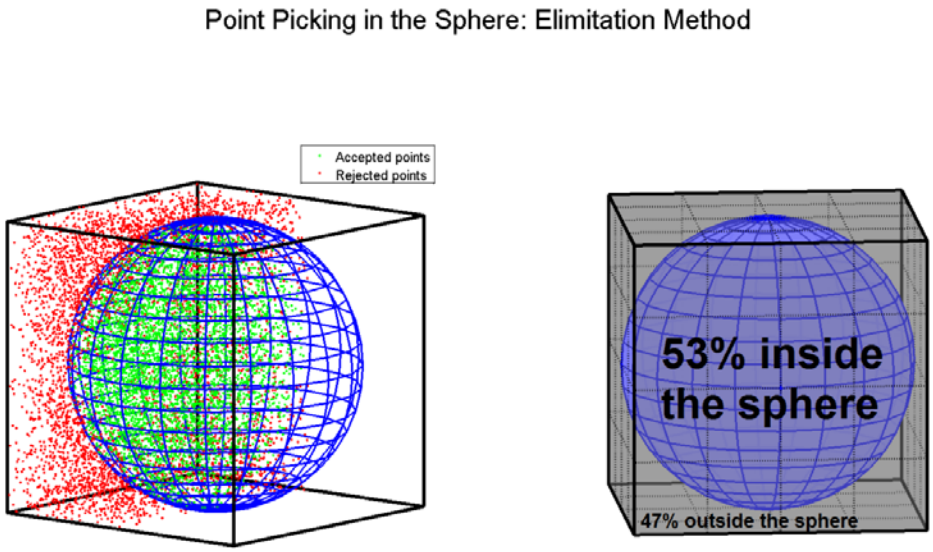

Fig. 8 Elimination method for point picking within the sphere. Points are generated within the smallest cubic region containing the sphere and then are rejected if they do not lie within the sphere. Only about 53% of points will be accepted with approximately 47% being rejected. For visual clarity, only points in the "back half" of the region are shown in the graph on the left.

3.2 Direct Method: The Most Common Mistake

As in the 2-dimensional (2-D) analogue, when point picking over the domain

$$S^2 := \{(x, y, z) \in \mathbb{R}^3 \mid x^2 + y^2 + z^2 \leq r^2\}, \tag{21}$$

most people will switch to spherical coordinates over the domain $[\rho, \theta, \varphi] \subseteq [0, r] \times [0, 2\pi] \times [0, \pi]$, attempt to draw each coordinate from a uniform distribution over its respective interval, and transform back to Cartesian coordinates using the standard transformations

$$x = \rho \ \cos\theta \ \sin\varphi \tag{22}$$

$$y = \rho \ \sin\theta \ \sin\varphi \tag{23}$$

$$z = \rho \ \cos\varphi. \tag{24}$$

Unfortunately, this once again produces clumped points; this time they appear to be clumped along the z-axis and most tightly at the origin (Fig. 9).

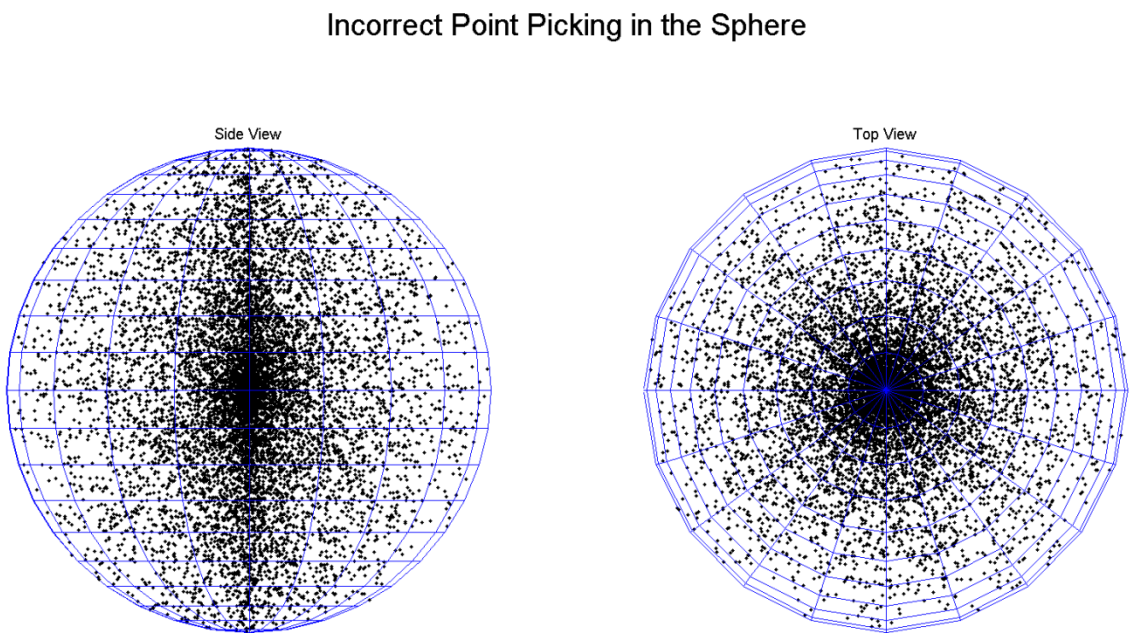

Fig. 9 Point picking within the sphere; drawing ρ-,θ-, and φ-coordinates from independent, uniform distributions over their respective domains yields a point distribution that is clumped along the z-axis and most tightly near the center of the sphere.

Again, although the density of ρ-coordinates over any change in ρ (i.e., over any $d\rho$), and the density of θ-coordinates over any change in θ (i.e., over any $d\theta$), and the density of φ-coordinates over any change in φ (i.e., over any $d\varphi$) remain the same, the volume of the resulting spherical quadrilateral (Fig. 10) is given by

$$dV = \rho^2 \ \sin\varphi \, d\rho \, d\theta \, d\varphi. \tag{25}$$

Equation 25 is commonly referred to as the volume element and should be familiar to anyone who has evaluated a triple integral in spherical coordinates.

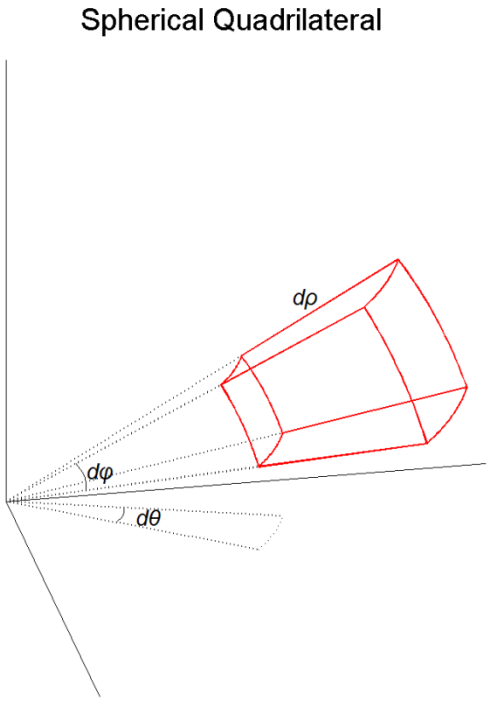

Fig. 10 Example of a spherical quadrilateral

This means that, for any 2 spherical quadrilaterals with equal $d\rho$s, $d\varphi$s, and $d\theta$s, the number of points within the spherical quadrilaterals will be the same. However, the volume, and therefore density, of points within each spherical quadrilateral will depend on both the ρ- and φ-coordinates of the spherical quadrilateral.

3.3 Direct Method: A Simple Transform

Luckily, the solution to the clumping problem in 3-D is similar to that in 2-D. We need only to find the appropriate coordinate transforms to remove the ρ- and φ-coordinate dependences from the volume of the spherical quadrilateral. In this case, we are looking for a coordinate transforms of the form

$$u = f(\rho), \quad f: [0, r] \to [a, b], \ f \in C^1 \tag{26}$$

$$v = g(\varphi), \quad g: [0, \pi] \to [c, d], \ g \in C^1 \tag{27}$$

such that

$$du = \rho^2 \, d\rho \tag{28}$$

and

$$dv = \sin\varphi \, d\varphi. \tag{29}$$

Then the volume element in Eq. 25 would become

$$dV = \rho^2 \sin\varphi \, d\rho \, d\varphi \, d\theta = du \, dv \, d\theta. \tag{30}$$

Note the change in order of integration. This is possible as we will now be integrating over a constant function with pairwise independent limits of integration.

Integrating Eqs. 28 and 29 yields the desired transforms

$$u = \tfrac{1}{3}\rho^3, \quad u: [0, r] \to \left[0, \tfrac{1}{3}r^3\right] \tag{31}$$

and

$$v = -\cos\varphi, \quad v: [0, \pi] \to [-1,1]\ . \tag{32}$$

For convenience, we can drop the constant coefficients and adjust the intervals to yield

$$u = \rho^3, \quad u: [0, r] \to [0, r^3] \tag{33}$$

and

$$v = \cos\varphi, \quad v: [0, \pi] \to [-1,1]. \tag{34}$$

Finally, in order to make use of these transforms, we take the inverse of Eq. 33 to yield

$$\rho = \sqrt[3]{u}, \quad \rho: [0, r^3] \to [0, r], \tag{35}$$

and make the following observation regarding Eq. 34:

$$\sin\varphi = \sqrt{1 - \cos^2\varphi} = \sqrt{1 - v^2}, \quad v \in [-1,1]. \tag{36}$$

With these coordinate transforms, the direct method for point picking within a sphere reduces to drawing u from a uniform $[0, r^3]$ distribution, v from a uniform $[-1, 1]$ distribution and θ from a uniform $[0,2\pi]$ distribution, and applying the transformations

$$x = \sqrt[3]{u}\,\sqrt{1 - v^2}\,\cos\theta\ , \tag{37}$$

$$y = \sqrt[3]{u}\,\sqrt{1 - v^2}\,\sin\theta\ , \tag{38}$$

and

$$z = \sqrt[3]{u}\,v. \tag{39}$$

The resulting points no longer exhibit the clumped distribution near the origin (Figs. 11 and 12), and it can be easily verified that the points are now uniformly distributed in x, y, and z (left to the reader).

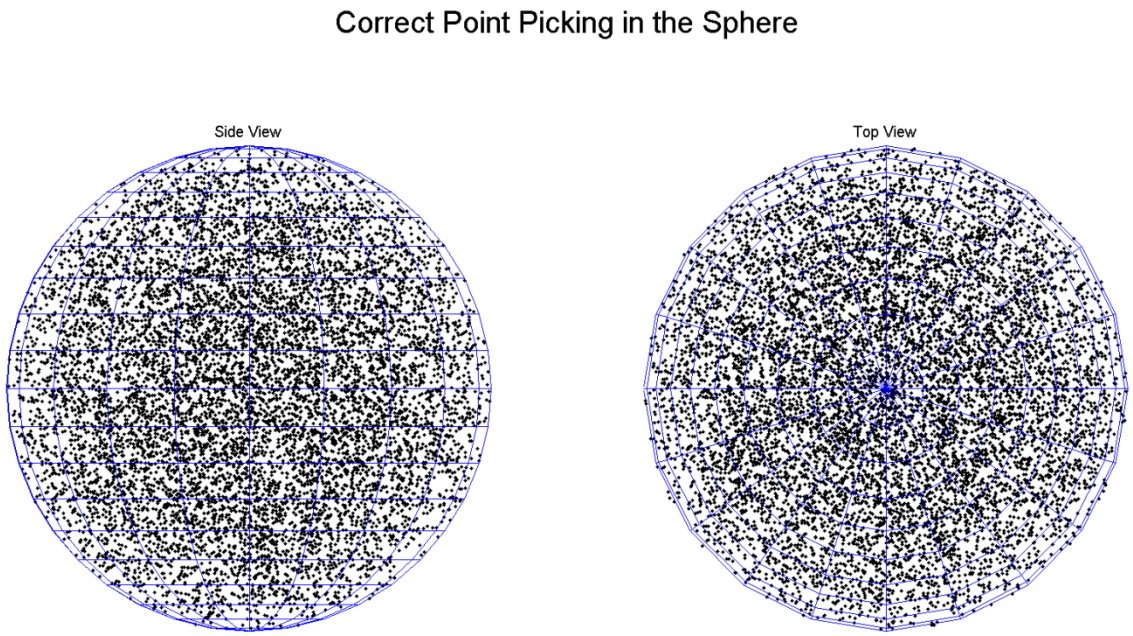

Fig. 11 Point distribution using the correct parameter domains and transformations. Notice the absence of the clumping problem.

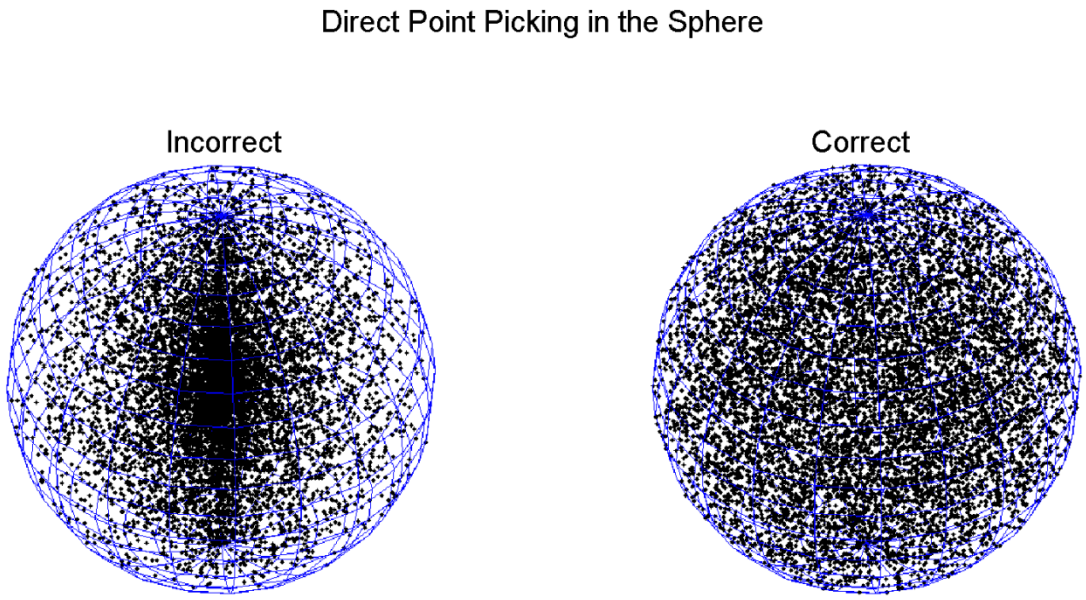

Fig. 12 Side by side comparison of the most common mistake and correct method for directly picking points within the sphere

3.4 Points on the Surface of the Sphere

Less trivial than its 2-D counterpart, one extension of the direct point picking method presented in Section 3.3 is picking uniformly distributed points on the surface of the sphere (Fig. 13). There are 2 common methods for achieving this.

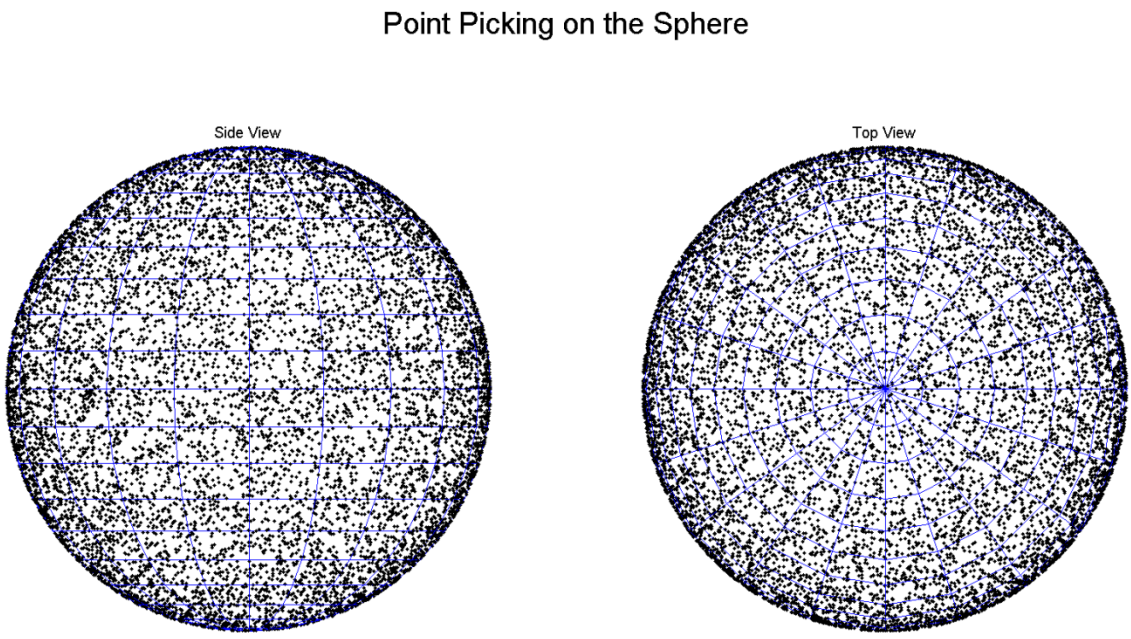

Fig. 13 Point picking on the sphere. Notice that the points appear to cluster around the image boundary in both views. This is due to the 2-D visualization of the points on the surface of the 3-D sphere.

The first is the projection method. In the projection method, the desired *n* points are first generated within the sphere using any method desired. The points are then projected onto the surface of the sphere by normalizing their Cartesian coordinates. This method is straightforward, intuitive, and simple to implement, but involves calculating the Euclidean norm of each point and dividing the x-, y-, and z-coordinates of each point by its respective norm.

The second method does not require any norm calculations or divisions and instead makes use of the equations from Section 3.3. The user need only note that the surface of the sphere is the set of points

$$\partial S^2 := \{(x, y, z) \in \mathbb{R}^3 \mid x^2 + y^2 + z^2 = r^2\}, \tag{40}$$

which is equivalent to the set

$$\Omega^2 := \left\{(\theta, \varphi) \in [0,2\pi] \times [0, \pi] \;\middle|\; \begin{matrix} x = r \sin\varphi \;\cos\theta \\ y = r \cos\varphi \;\cos\theta \\ z = r \cos\varphi \end{matrix}\right\}. \tag{41}$$

Therefore, the direct method for point picking on the surface of a sphere of r reduces to drawing v from a uniform $[-1, 1]$ distribution and θ from a uniform $[0,2\pi]$ distribution and applying the transformations

$$x = r\sqrt{1 - v^2}\,\cos\theta\,, \tag{42}$$

$$y = r\sqrt{1 - v^2}\,\sin\theta\,, \tag{43}$$

and

$$z = rv. \tag{44}$$

4. Point Picking on an *N*-Sphere

An alternate method for point picking on the surface of the sphere is presented here as a general method that extends to higher dimensions. This general method, which we will call Muller's method, is presented without proof, and the reader is directed to the specified references for insight and proof for the validity of this method.

Muller's method[4,5] is a 2-step process for uniformly generating points on the boundary of the *N*-sphere,

$$S^N := \{x = (x_1, x_2, \dots, x_{N+1}) \in \mathbb{R}^{N+1} \,\big|\, \textstyle\sum_{k=1}^{N+1} x_k^2 = r^2\}. \tag{45}$$

Step 1: Generate *N* independent standard normal random variables, y_k, $k = 1, \dots, N + 1$.

Step 2: Construct the point

$$x = (x_1, x_2, \dots, x_{N+1}) \tag{46}$$

where

$$x_k = \left({}^{r}\!/_{\|y\|}\right) y_k, \quad k = 1, \dots, N + 1 \tag{47}$$

and

$$\|y\| = (\textstyle\sum_{k=1}^{N+1} y_k^2)^{1/2}. \tag{48}$$

Figure 14 shows points generated by Muller's method for $N = 2$. It can be easily verified that these points are uniformly distributed over the surface of the sphere (left to the reader).

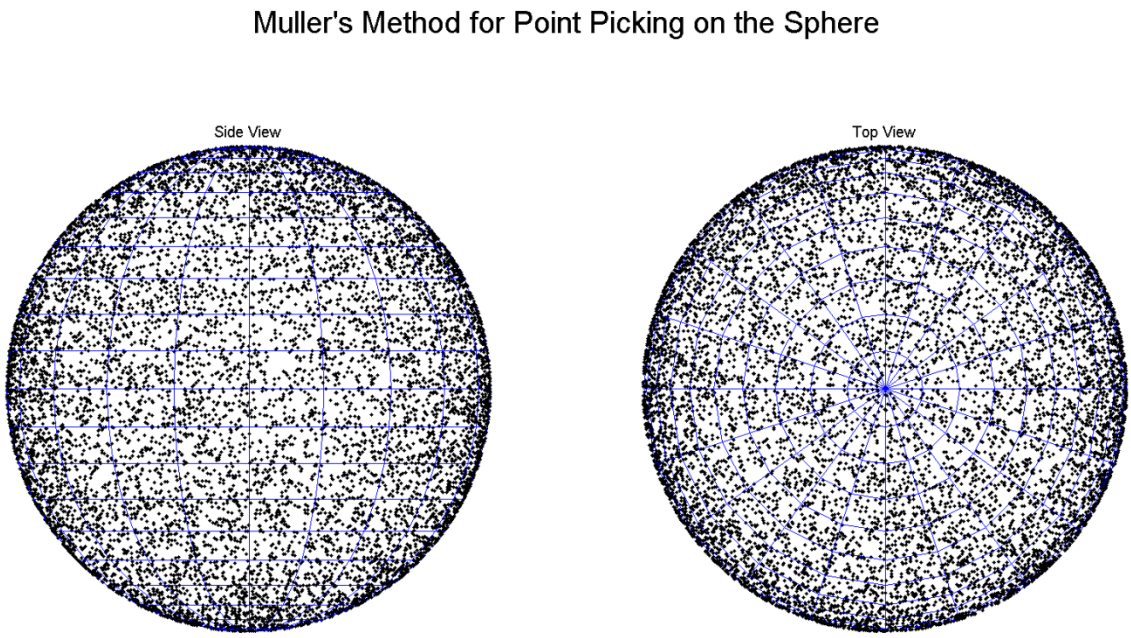

Fig. 14 Point picking on the sphere using Muller's Method. Notice that the points appear to cluster around the image boundary in both views. This is due to the 2-D visualization of the points on the surface of the 3-D sphere. This distribution appears to be equivalent to that generated with the direct method presented in Section 3.4. The distributions are truly equivalent, and the proof is left to the reader.

5. Evenly Spaced Points on a Disc

Algorithms presented in this section for evenly distributing points across a disc are not optimal solutions. In fact, the concept of what it means to be an evenly spaced distribution is not going to be formally defined. Instead, we offer a "visual definition" in the form of 2 graphs in Fig. 15. The points in the graph on the left are not evenly spaced, while those in the graph on the right are evenly spaced.

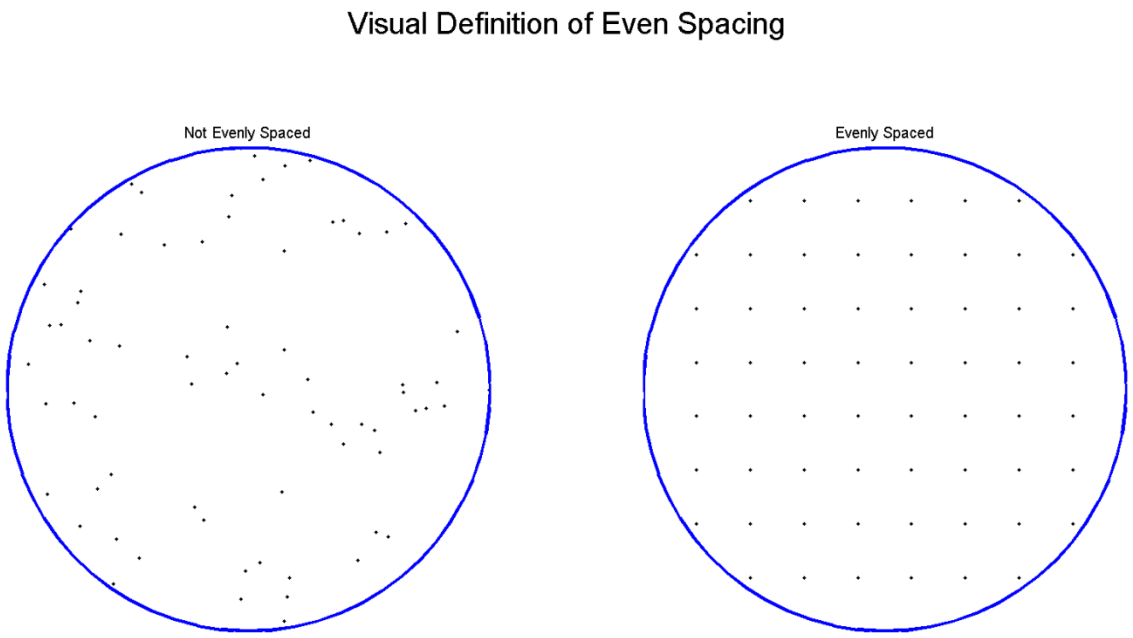

Fig. 15 Visual definition of what it means for points to be "evenly spaced". The points within the circle on the left are not evenly spaced. The points within the circle on the right are evenly spaced.

There are many methods that will produce more evenly spaced points than those presented in this report, but those methods often come at a significant computational cost. Many of these methods involve treating a set of points as particles confined to the disc, and minimizing the forces between the particles. Especially as the number of particles increases, such an optimization problem can become computationally impractical. Instead, we look for approximate methods that only involve algebraic expressions.

When attempting to evenly distribute n points across the surface of a disc of radius r using only algebraic equations, a common first idea is to employ some form of spiral algorithm. In fact, there are entire families of spirals that work very well for this purpose. One of the most useful families of spirals are the Archimedean spirals. In polar coordinates, Archimedean spirals all have the form

$$\rho = a + b\theta^{1/c}, \quad a, b \in \mathbb{R}, c \in \mathbb{R}\backslash\{0\}. \tag{49}$$

The following sections describe how to use 2 subfamilies of Archimedean spirals, along with the help of the spiral of Theodorus, to produce evenly spaced point distributions on a disc of radius r.

5.1 Single Spiral Method: Archimedes and Theodorus

The idea behind the single spiral method is to construct a sequence of n points along a single spiral that starts at the origin, winds out toward the disc's boundary, and has the following properties:

1. The distance between any 2 successive points along the spiral is constant.
2. The distance between any 2 successive windings of the spiral is constant.
3. The distance between any 2 successive points along the spiral is as close as possible to the distance between any 2 successive windings of the spiral.

Archimedes's spiral (Fig. 16) is the name for the case when $c = 1$ in Eq. 49. Archimedes's spiral exhibits the useful characteristic that the distance between any 2 successive windings along any ray emanating from the origin is constant (Fig. 17). In fact, this distance is known exactly, and has the equation

$$d = 2\pi b. \tag{50}$$

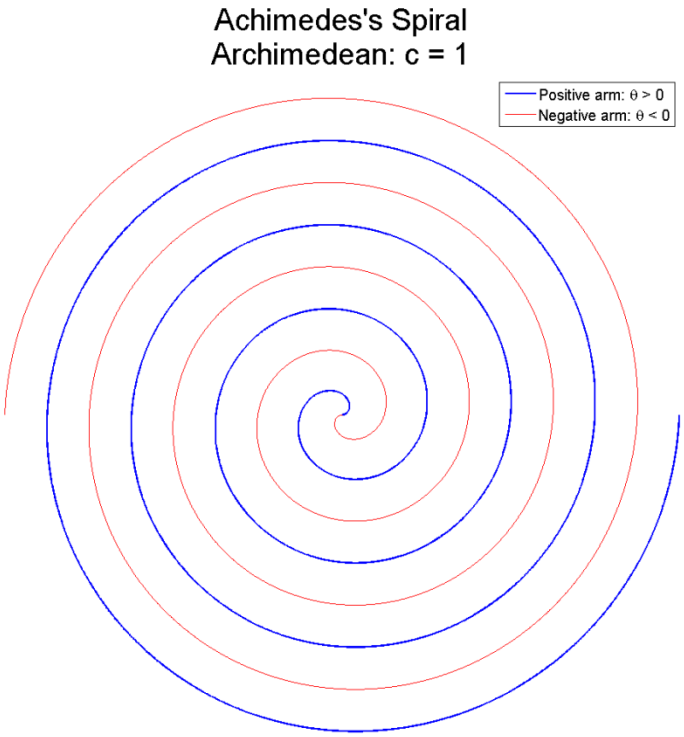

Fig. 16 Archimedes's spiral is the Archimedean spiral given by $\rho = a + b\theta$, where $a, b \in \mathbb{R}$

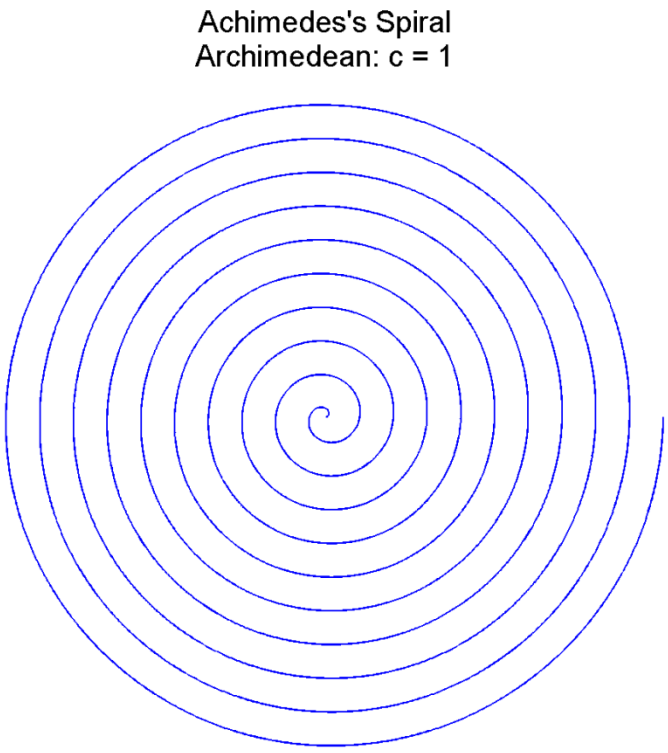

Fig. 17 A useful characteristic of Archimede's spiral is that the distance between any 2 successive windings is constant. Only the positive arm is shown; only one arm of the spiral was needed to derive the single spiral method, and the positive arm was chosen arbitrarily.

This characteristic satisfies property (2) and makes Archimedes's spiral an ideal contender for constructing our single spiral point distribution. The next step is to pick a and b, and either ρ or θ in such a way that the distance between any 2 successive points along the spiral is constant.

The spiral of Theodorus is a spiral that was first constructed by the Greek mathematician Theodorus of Cyrene in the 5th century BCE.[6] The spiral of Theodorus starts with an isosceles right triangle and is formed by a sequence of contiguous right triangles such that hypotenuse of each triangle become the longer cathetus (i.e., the longer nonhypotenuse side) of each successive triangle (Fig. 18). A very useful characteristic of the spiral of Theodorus is that the Euclidean distance between any 2 successive vertices of the spiral is constant.

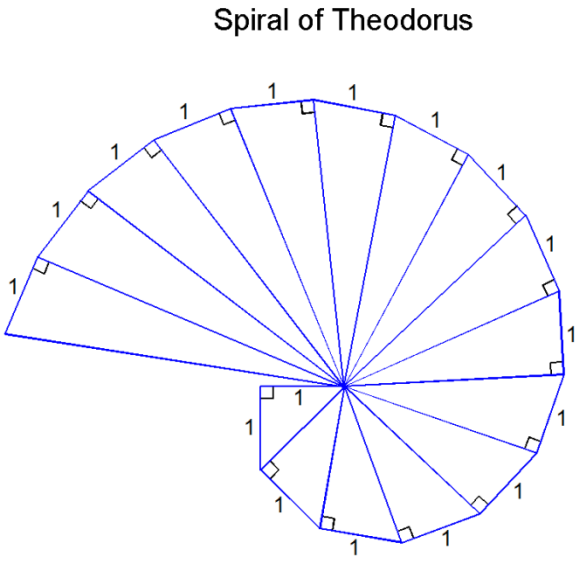

Fig. 18 The spiral of Theodorus, also known as the square root spiral, Einstein spiral, or Pythagorean spiral

Similar to Archimedes's spiral, the spiral of Theodorus exhibits the characteristic that the distance between any 2 successive windings along any ray emanating from the origin is nearly constant (Fig. 19). Although, this does not exactly satisfy property (2), the distance between any 2 successive winding monotonically approaches the value of π from above very rapidly. Furthermore, as $n \to \infty$, the spiral of Theodorus happens to be an extremely close approximation to Archimedes's spiral with the equation

$$\rho = \frac{1}{2}(\theta - 1)\ . \tag{51}$$

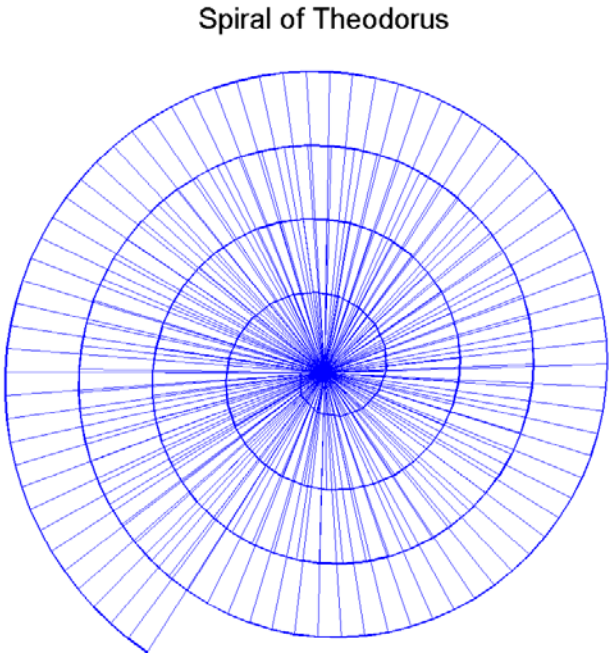

Fig. 19 Similar to Archimedes's spiral, the distance between successive windings of the spiral of Theodorus is nearly constant

These 2 spirals together provide all the tools we need to construct a single spiral of n points that satisfies our properties (1), (2), and (3).

Starting with the sequence of hypotenuses from the spiral of Theodorus as the radial coordinates, we form the sequence of points

$$\left(p_k = (\rho_k, \theta_k) = \left(\sqrt{k}, \theta_k\right)\right)_{k=1}^{n}. \tag{52}$$

At this point, the angular components in the sequence are completely unknown. We then break the structure of the spiral of Theodorus by adjusting the "winding constant", the coefficient of θ in Eq. 49, until property (3) is satisfied. In other words, we are going to look for Archimedes's spiral such that the distance between consecutive windings is as close as possible to the distance between points with consecutive ρ-values from Eq. 52. More precisely, we are looking for an equation of the form

$$\theta = \frac{1}{b}\rho, \quad b \in \mathbb{R}^+ \tag{53}$$

such that

$$distance(p_k,\ p_{k+1}) = 2\pi b. \tag{54}$$

Expanding Eq. 54 in polar coordinates yields

$$\sqrt{{\rho_k}^2 + {\rho_{k+1}}^2 - 2\,\rho_k\,\rho_{k+1}\,\cos(\theta_{k+1} - \theta_k)} = 2\,\pi b. \tag{55}$$

Substituting Eq. 53 into Eq. 55 and simplifying yields

$$\rho_k{}^2 + \rho_{k+1}{}^2 - 2\,\rho_k\,\rho_{k+1}\,\cos\left(\frac{\rho_{k+1}-\rho_k}{b}\right) = 4\,\pi^2 b^2. \tag{56}$$

Finally, substituting Eq. 52 into Eq. 56 and simplifying yields the relationship

$$2k + 1 - 2\,\sqrt{k}\,\sqrt{k+1}\,\cos\left(\frac{\sqrt{k+1}-\sqrt{k}}{b}\right) = 4\,\pi^2 b^2. \tag{57}$$

Although it may not be apparent, taking the limit as $k \to n$ and $n \to \infty$ of the left hand side of the equation reveals the solution (see the Appendix for full limit evaluation)

$$\lim_{n\to\infty}\lim_{k\to n} 2k + 1 - 2\,\sqrt{k}\,\sqrt{k+1}\,\cos\left(\frac{\sqrt{k+1}-\sqrt{k}}{b}\right) = \frac{1}{4b^2}. \tag{58}$$

Therefore, as $k \to n$ and $n \to \infty$, Eq. 57 becomes

$$\frac{1}{4b^2} = 4\,\pi^2 b^2, \tag{59}$$

and we are left with the desired turning parameter

$$b = \frac{1}{2\sqrt{\pi}}. \tag{60}$$

Putting Eqs. 52, 53, and 60 together produce the sequence of points

$$\left(p_k = (\rho_k, \theta_k) = \left(\sqrt{k}, 2\sqrt{\pi k}\right)\right)_{k=1}^{n}, \tag{61}$$

which satisfy all 3 desired properties. However, these points cover a disc of radius $\sqrt{n}$ instead of a disc of the desired radius *r*. The final step is to introduce a radial scale factor

$$\rho_k = t\sqrt{k}, \quad t \in \mathbb{R}^+ \tag{62}$$

and impose the radial constraint

$$\rho_n = r. \tag{63}$$

Eqs. 62 and 63 uniquely determine a value $t = \frac{r}{\sqrt{n}}$, and produce the sequence of ρ-values

$$\left(\rho_k = r\sqrt{\frac{k}{n}}\right)_{k=1}^{n}. \tag{64}$$

Since scaling the radial component of a set of points in polar coordinates by a constant value scales the pair-wise distances between points by that value, scaling the ρ-values this way not only scales the distance between successive windings by a constant value, but it also scales the distance between successive points on the spiral by the same amount. So Eqs. 61 and 64 produce the desired sequence of points

$$\left(p_k = (\rho_k, \theta_k) = \left(r\sqrt{\frac{k}{n}}, 2\sqrt{\pi k}\right)\right)_{k=1}^{n}. \tag{65}$$

Figure 20 shows 10,000 evenly spaced points generated by the single spiral method.

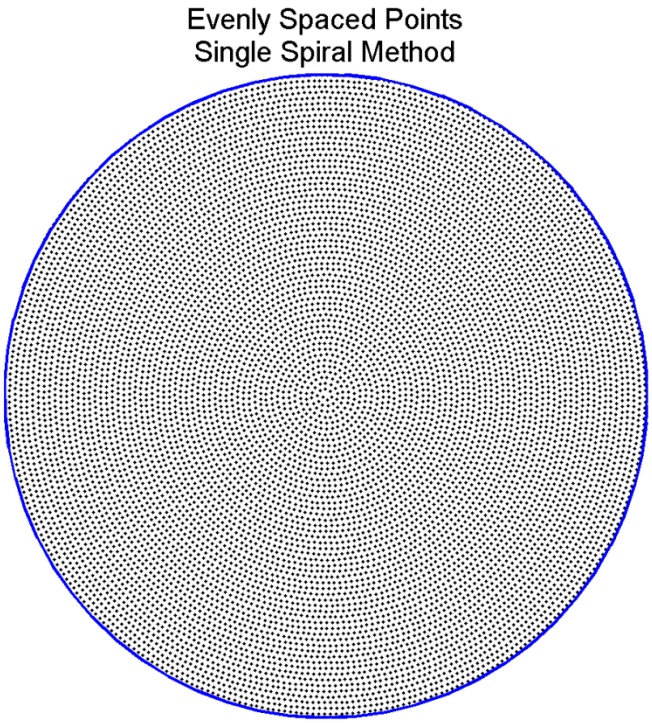

Fig. 20 Ten thousand evenly spaced points on a disc generated by the single spiral method

5.2 Single Spiral Method Revisited: Fixing the Center Point

Although the sequence of points formed from Eq. 65 produce a fairly uniform covering of the disc, the reader may notice in practice that this method always leaves a bit of a blank space near the center of the of disc. The following equations are provided as "patch" to fill this space. This "patch" was developed solely by trial and error, but the method appears to work well in practice for any value of *n*.

$$\left(p_k = (\rho_k, \theta_k) = \left(r\sqrt{\frac{k}{n-1}}, 2\sqrt{\pi k}\right)\right)_{k=1}^{n-1} \tag{66}$$

$$p_0 = (\rho_0, \theta_0) = \left(\frac{2}{3}\,\rho_1, \frac{1}{2}\theta_1\right) = \left(\frac{2r}{3}\sqrt{\frac{1}{n-1}}, \sqrt{\pi}\right). \tag{67}$$

Figure 21 shows the patch for 2 values of *n*.

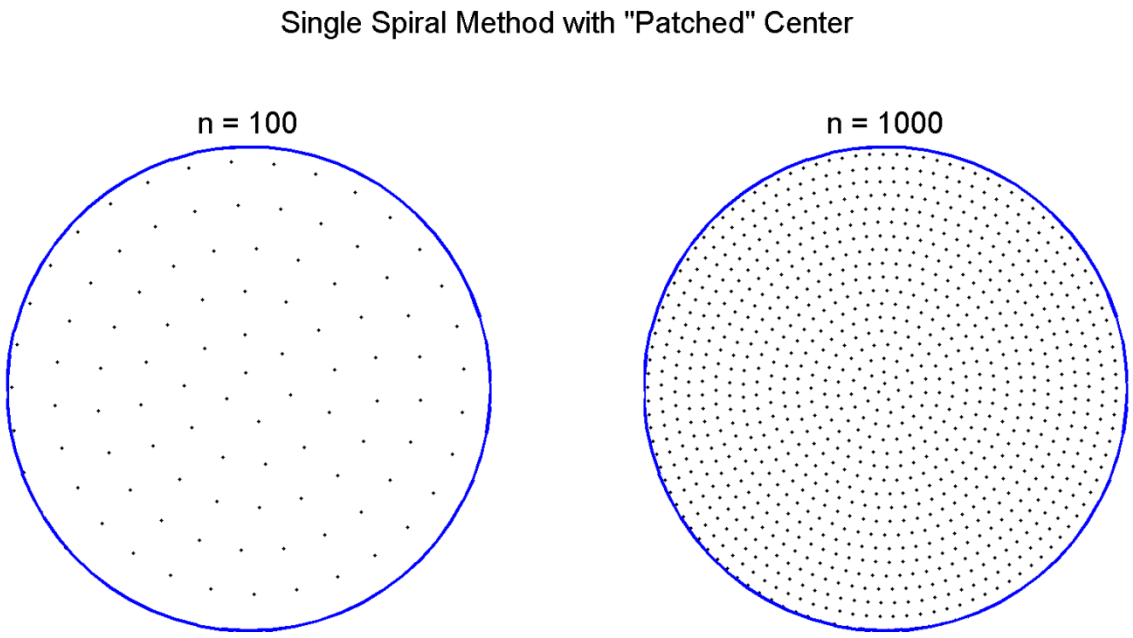

Fig. 21 Single spiral method with “center” point adjusted to better fill the space

From this point on, any reference to the single spiral method refers to this “patched” single spiral method.

5.3 Vogel’s Method: Fermat

Quite often, nature does it best. Consider the head of the sunflower (Fig. 22), the seeds of which are evenly distributed over the “disc”. Extensive research regarding the pattern formed by the seeds in the head of a sunflower exists for the interested reader, but for the purpose of this report, we acknowledge the spiral phenomena and focus on an implementation of some work done by Helmut Vogel.[7] Vogel suggested the use of Fermat’s spiral,[8] the case when $c = 2$ in Eq. 49 instead of the commonly used logarithmic spiral to model the pattern of the seeds on the head of a sunflower (Fig. 23).

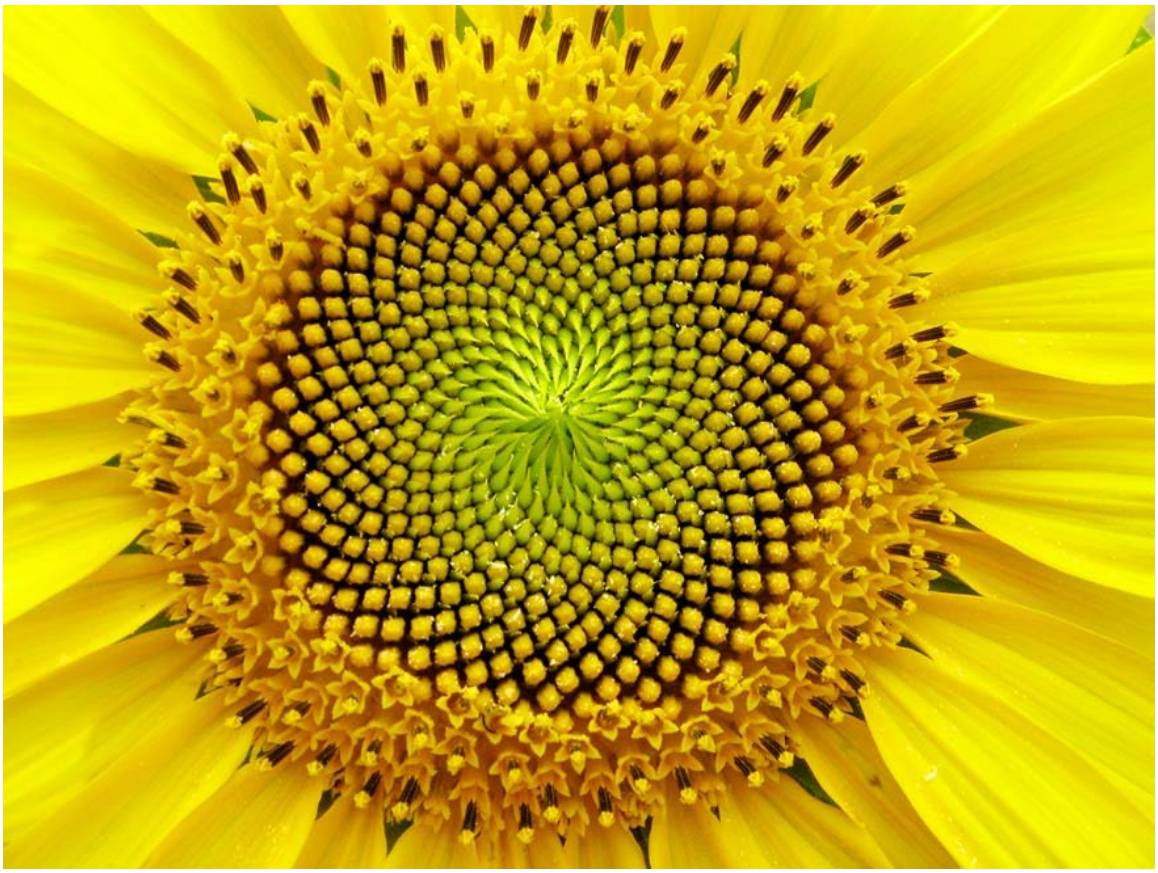

Fig. 22 Spirals can be found all over the natural world such as in the arrangement of seeds on the head of a sunflower

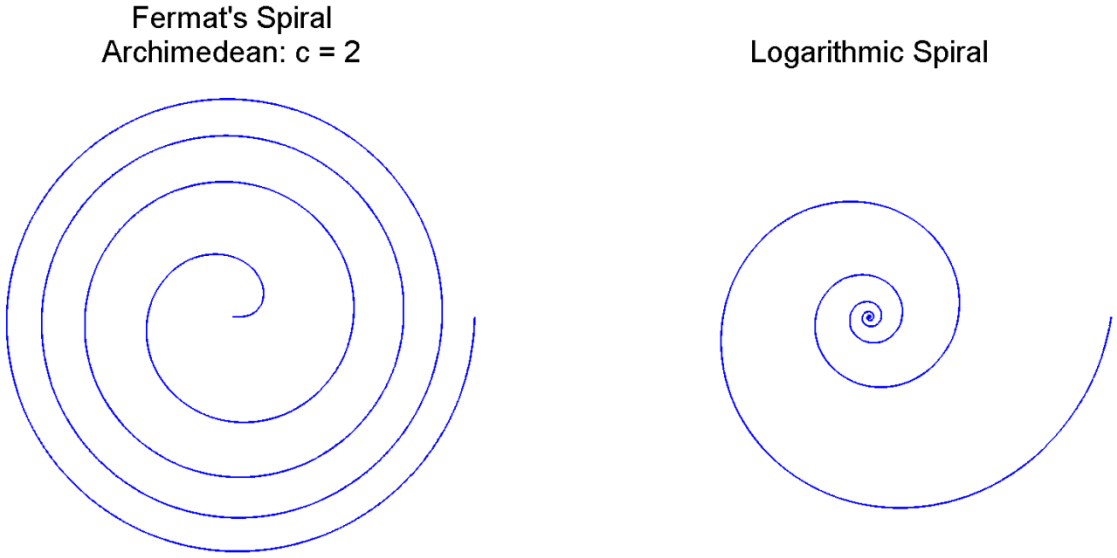

Fig. 23 Both logarithmic and Fermat's spirals can be used to model the observed spiral of seeds on the head of a sunflower

Vogel's model then has the form

$$\theta_k = k * \delta \tag{68}$$

and

$$\rho_k = t\sqrt{k}, \in \mathbb{R}^+ , \tag{69}$$

where δ is the golden angle. The golden angle is related to the golden ratio, $\varphi = \frac{1+\sqrt{5}}{2}$, by the equation

$$\delta = 2\pi\left(1 - \frac{1}{\varphi}\right) = \pi\left(3 - \sqrt{5}\right), \tag{70}$$

where the golden ratio is the limit of the ratios of successive terms in the Fibonacci sequence.

Again imposing the radial constraint in Eq. 63, we arrive at the final form of what we will call Vogel's method[9]

$$\left(p_k = (\rho_k, \theta_k) = \left(r\sqrt{\frac{k}{n}},\ \pi\left(3 - \sqrt{5}\right)(k-1)\right)\right)_{k=1}^{n} . \tag{71}$$

Figure 24 shows 10,000 evenly spaced points generated by Vogel's method.

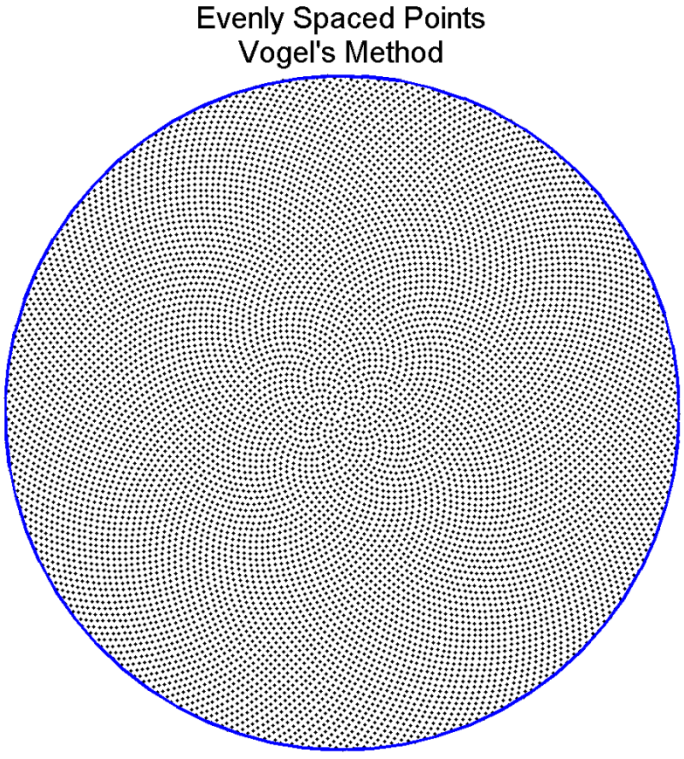

Fig. 24 Ten thousand evenly spaced points on a disc generated by Vogel's method

5.4 Spiral Method Comparison

The question must now be asked: Is one spiral method better than the other? Unfortunately, there is no clear answer, especially as we have avoided formally defining what it means to be a "good" method for generating evenly spaced points. One possible metric that can be used to compare these (and other) methods for generating evenly spaced points is the standard deviation in the size of the cells of the Voronoi diagram of the points. A Voronoi diagram is a partitioning of the plane into convex polygons with respect to a set of vertices (one vertex per cell) such that any point within a given cell is closer to that cell's vertex than it is to any other vertex. So while the average area of any partitioning of S^1 into n regions will always be $\pi * r^2/n$, the standard deviation of the area of regions can provide insight into how much the sizes of the regions vary.

Figure 25 shows Voronoi diagrams and standard deviation of cell area for both spiral methods for 500 points. Although both methods produce distributions of points that appear to be fairly evenly spaced, the standard deviation of the area of Voronoi cells of Vogel's method is slightly more than 28% less than that of the single spiral method. This indicates that Vogel's method produces a more evenly spaced set of points as measured by the stated metric.

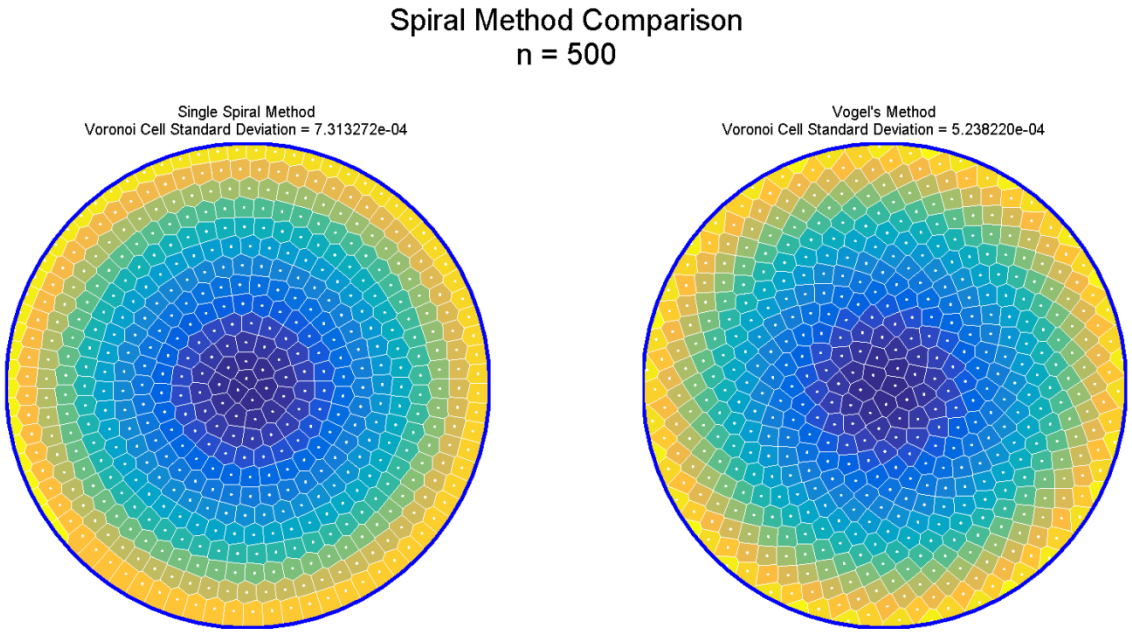

Fig. 25 Voronoi diagram comparison of single spiral and Vogel's method for generating evenly spaced points on a disc

6. Evenly Spaced Point Distribution on a Sphere

The problem of "evenly spacing" *n* points on the surface of the sphere was first proposed by JJ Thomson in 1904.[10] In his paper, Thomson was looking to determine equilibrium configurations of electrons constrained to the surface of a sphere and subject to Coulomb's inverse-square law. This problem became known as Thomson's problem. To this day, although the solutions to a handful of special cases are known, there is no general solution for *n* electrons to Thomson's problem.

In 1942, László Fejes Tóth began studying a similar problem of maximizing the minimum pair-wise distance between *n* points on the unit sphere.[11] This problem became known as Fejes Tóth's problem. In 1943, Fejes Tóth proved that for any *n* points, there will always exist 2 points such that the distance, *d*, between them satisfies the inequality

$$d \leq \sqrt{4 - \csc^2\left(\frac{\pi\, n}{6\,(n-2)}\right)}. \tag{72}$$

Furthermore, Fejes Tóth showed that this limit is exact for *n* = 3, 4, 6, and 12; but like Thomson's problem, Fejes Tóth's problem has no known general solution.

So here we have presented 2 approaches to the problem of finding an "even spacing" of *n* points on the surface of the sphere; but as Whyte (1952) points out, Thomson's problem and Fejes Tóth's problems do not have the same solution for general *n*. As in 2-D analogue of the previous section, we now state that the algorithms presented in this section are not exact, or even optimal, solutions for producing evenly spaced distributions of points on the surface of the sphere. This is a direct result of both the fact that there is more than one formulation of the problem of "evenly spacing" *n* points on the surface of the sphere (we presented 2 formulations that are known to not be equivalent), and that there was still no known general solution to any such formulation at the time of this report.

In fact, only the vertices of the 5 Platonic solids can be said to be truly evenly spaced around the surface of a sphere. A Platonic solid is any regular, convex polyhedron with congruent faces of regular polygons and the same number of faces meeting at each vertex. Therefore, vertices of the Platonic solids are perfectly evenly spaced[12] by definition (Fig. 26). However, there are only 5 such convex polyhedra.[13]

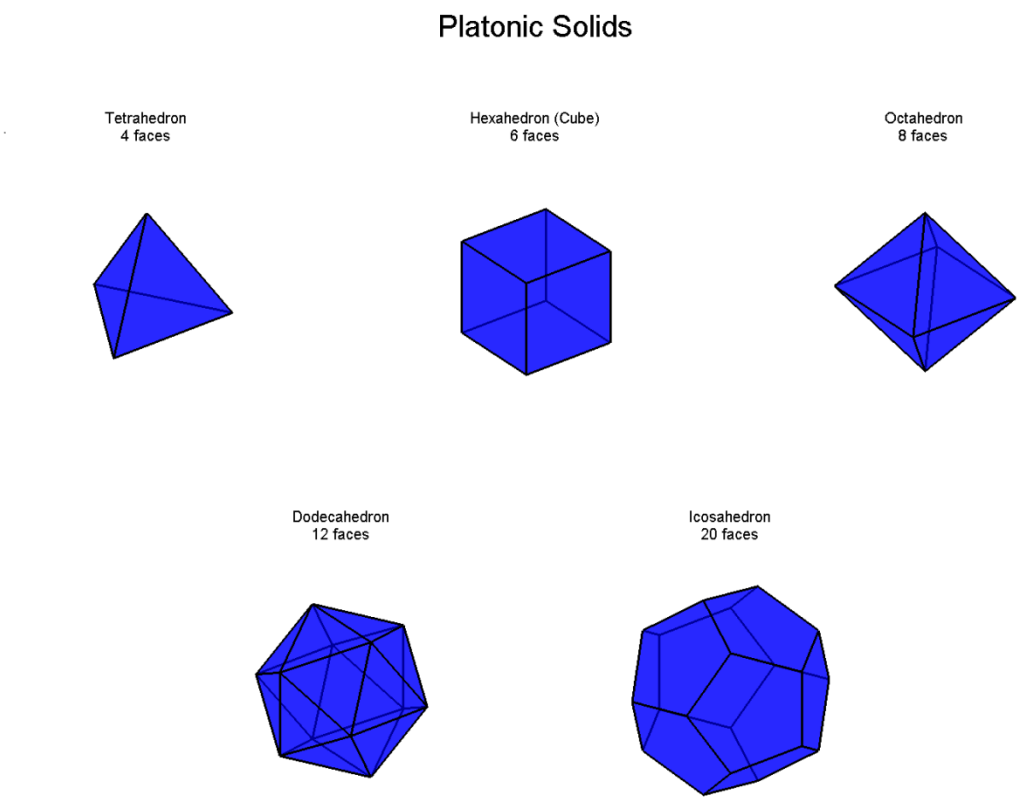

Fig. 26 The 5 Platonic solids, i.e., the only truly evenly spaced point distributions over the surface of the sphere

It is for these reasons that we again forego formally defining the concept of what it means to be an evenly spaced distribution. Instead, we offer another “visual definition” in the form of 2 graphs in Fig. 27. The points in the graph on the left are not evenly spaced, while those in the graph on the right are evenly spaced.

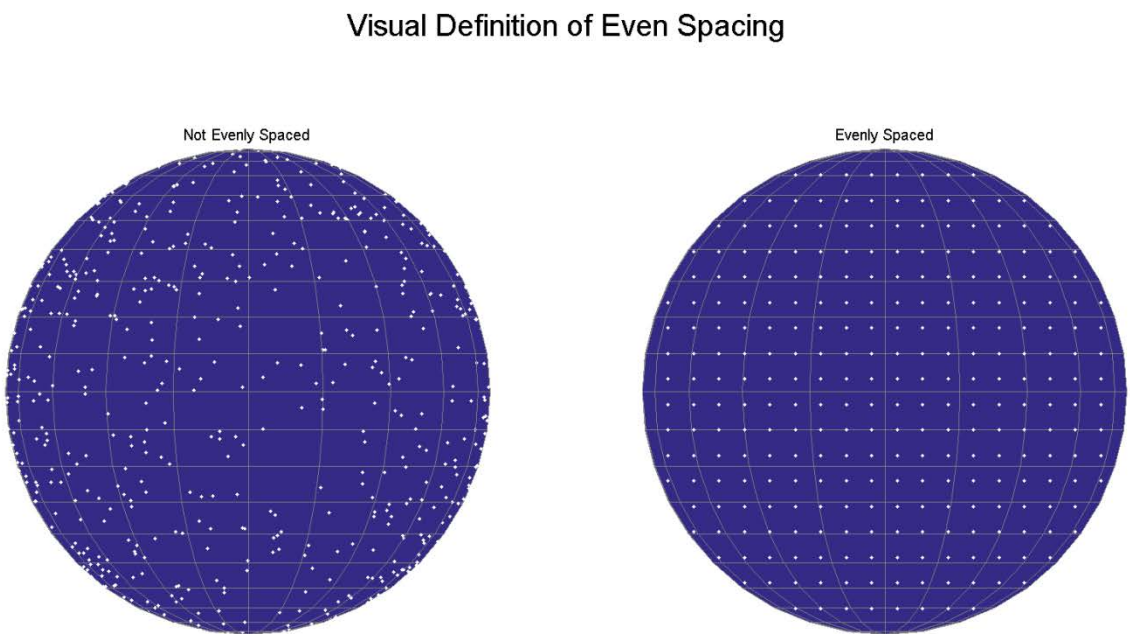

Fig. 27 Visual definition of what it means for points to be "evenly spaced". The points on the surface of the sphere on the left are not evenly spaced. The points on the surface of the sphere on the right are evenly spaced.

When evenly spacing points over the surface of the sphere, 3 of the most common techniques are electrostatic repulsion, geodesic subdivision, and spiral methods. Electrostatic repulsion is essentially Thomson's problem; place *n* points anywhere on the surface of the sphere, simulate the repelling forces between the points, and look for a stable (i.e., converged) configuration.

With geodesic subdivision, start with an octahedron (8 congruent triangular faces) or icosahedron (20 congruent triangular faces), place a point at the midpoint of each edge and normalize the coordinates of each new point to "push" it out to the surface of the sphere, and keep repeating until the desired number of points is attained. Each geodesic subdivision transforms each triangular face into 4 triangular faces, but as it involves a projection to the surface of the sphere, it also breaks the congruency of the faces. An interesting application of geodesic subdivision is the design of domes, buildings, and structures (e.g., Spaceship Earth[14] at Epcot, Walt Disney World; the Long Island Green Dome[15] in Calverton, NY; the Montréal Biosphère[16] in the former pavilion of the United States for the 1967 World Fair Expo 67 at Parc Jean-Drapeau in Montréal, Québec; and the Climatron[17] at the Missouri Botanical Garden in St. Louis, MO). Geodesic subdivision only works for configurations of points where

$$n = 2 + 4^k, \quad k \in \mathbb{Z}^+ \tag{73}$$

or

$$n = \frac{1}{2}(4 + 5 * 2^{2k}), \quad k \in \mathbb{Z}^+. \tag{74}$$

Configurations with the number of points given by Eq. 73 are created by starting geodesic subdivision with an octahedron. Configurations with the number of points given by Eq. 74 are created by starting geodesic subdivision with an icosahedron.

As in the 2-D analogue, spirals are a natural structure for distributing points over the surface in question. Just as electrostatic repulsion, geodesic subdivision, and spiral methods are not the only 3 methods for distributing points on the surface of the sphere, the following spiral methods are neither an exhaustive set nor do they claim to be the "best" methods. Instead, the spiral methods presented were chosen for their balance of ease of use and overall performance.

6.1 Rakhmanov, Saff, and Zhou

In 1994, Rakhmanov, Saff, and Zhou were concerned with what is commonly referred to as the extremal energy for *n* points on the sphere. To discuss the extremal energy, we first need some notation and definitions. From this point on, all calculations are for points on the unit sphere. Scaling the points to spheres of different radii is straightforward and left to the reader.

For $n \in \mathbb{Z}$, $n > 2$, let $\omega_n = \{x_1, \ldots, x_n\}$ be a set of *n* points on the unit sphere

$$\Omega S_1^2 := \{(x, y, z) \in \mathbb{R}^3 \mid x^2 + y^2 + z^2 = 1\}. \tag{75}$$

Then for each $\alpha \in \mathbb{R}$, the α–energy associated with ω_n is defined by

$$E(\alpha, \omega_n) := \begin{cases} \sum_{1 \le i < j \le n} \log \frac{1}{|x_i - x_j|}, & \alpha = 0 \\ \sum_{1 \le i < j \le n} \left|x_i - x_j\right|^{\alpha}, & \alpha \neq 0 \end{cases}, \tag{76}$$

and the extremal energy for *n* points on ΩS_1^2 is defined by

$$\mathcal{E}(\alpha, n) := \begin{cases} \inf\limits_{\omega_n \subset \Omega S_1^2} E(\alpha, \omega_n), & \alpha \le 0 \\ \sup\limits_{\omega_n \subset \Omega S_1^2} E(\alpha, \omega_n), & \alpha > 0 \end{cases}. \tag{77}$$

The problem of determining the extremal energy can be thought of a generalization of both Thomson's and Feje Tóth's problems. In this notation, Thomson's problem seeks to determine the extremal energy when $\alpha = -1$, i.e., seeks to determine $\mathcal{E}(-1, n)$; Feje Tóth's problem seeks to determine the extremal energy when $\alpha = 1$ [i.e., seeks to determine $\mathcal{E}(1, n)$].

Rakhmanov, Saff, and Zhou were not specifically interested in any one value of α, but were looking to provide bounds for the discrete extremal energy for $-2 < \alpha < 2$. Furthermore, they sought a simple explicit formula for distributing *n* points on the surface of the sphere that would closely estimate $\mathcal{E}(\alpha, n)$.

The reader is directed to their 1994 paper[18] for the details of these bounds, while the equations for what Rakhmanov, Saff, and Zhou called generalized spiral points are presented in the following

equations. The θ and φ variables have been switched from that presented in Rakhmanov, Saff, and Zhou to conform to spherical coordinate notation used throughout this report.

For any $n \in \mathbb{Z}$, define the sequence

$$h_k := 1 - \frac{2\,(k-1)}{n-1},\ 1 \le k \le n. \tag{78}$$

Then $\widehat{\omega}_n = \{(\theta_k, \varphi_k)\}_{k=1}^{n} \subset [0, 2\pi] \times [0, \pi]$ denotes the generalized spiral on ΩS_1^2 in spherical coordinates ($\rho = 1$), and is defined as

$$\theta_1 := \theta_n := 0, \tag{79}$$

$$\theta_k := \left(\theta_{k-1} + \frac{C}{\sqrt{n}} \frac{1}{\sqrt{1-h_k^2}} \right) mod\ (2\pi),\ 2 \le k \le n-1, \tag{80}$$

and

$$\varphi_k := \cos^{-1}(h_k), \tag{81}$$

where C is a constant chosen such that successive points will all be approximately the same distance apart on ΩS_1^2. Rakhmanov, Saff, and Zhou found that $C = 3.6$ worked well for $n \le 12{,}000$. Rakhmanov, Saff, and Zhou's (RSZ) spiral with 1,000 points is shown in Fig. 28.

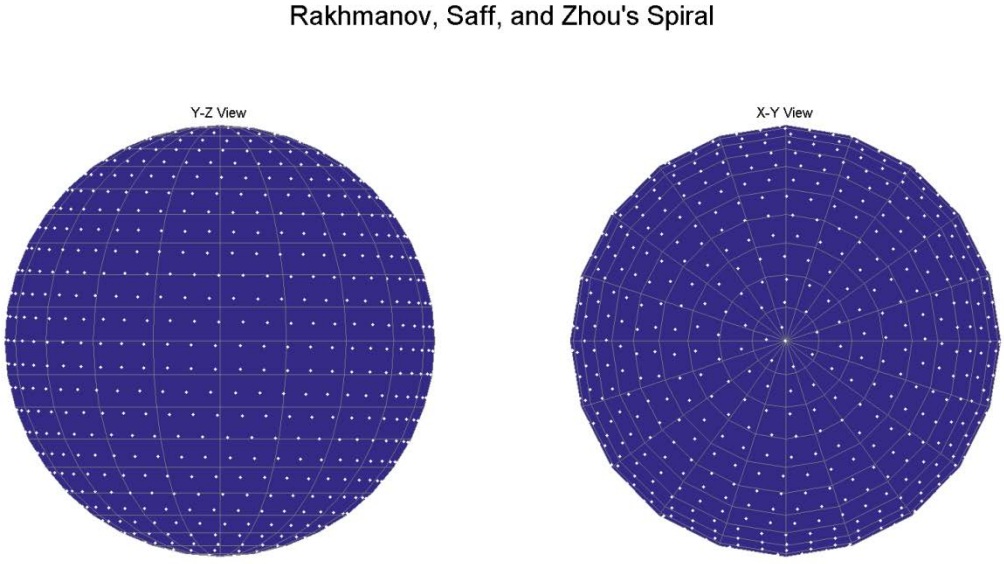

Fig. 28 One thousand points of Rakhmanov, Saff, and Zhou's spiral on the surface of a sphere

6.2 Rakhmanov, Saff, and Zhou: 2 Improved Variations

While an RSZ spiral looks to cover the sphere with fairly evenly spaced points, it can be easily seen that the spacing is less than optimal at the 2 poles. However, there is a very simple

adjustment that can be made to a standard RSZ spiral to address the points in question. Basically, we shift the first and last points, p_0 and p_{n-1}, away from the poles and recalculate the spacing of the intermediate points. For the sake of fast and efficient implementation, the following equivalent set of equations for an RSZ spiral is first offered without proof:

$$s = \frac{3.6}{\sqrt{n}}, \tag{82}$$

$$dz = \frac{2}{n-1}, \tag{83}$$

$$z_k = 1 - k * dz, \qquad 0 \le k \le n-1, \tag{84}$$

$$r_k = \sqrt{1 - z_k^2}, \qquad 0 \le k \le n-1, \tag{85}$$

$$\theta_k = k * s, \qquad 0 \le k \le n-1, \tag{86}$$

$$x_k = r_k \cos(\theta_k), \qquad 0 \le k \le n-1, \tag{87}$$

$$y_k = r_k \sin(\theta_k), \qquad 0 \le k \le n-1. \tag{88}$$

Then the RSZ spiral adjustment for addressing the points at the poles can be accomplished by choosing a slightly different value of dz in Eq. 83 while shifting the values of z_k in Eq. 84 as follows:

$$dz = \frac{2}{n} \tag{89}$$

and

$$z_k = 1 - \left(k + \frac{1}{2}\right) * dz, \quad 0 \le k \le n-1. \tag{90}$$

Eqs. 82 and 85–88 remain the same, and the spiral is appropriately adjusted as can be seen in Fig. 29.

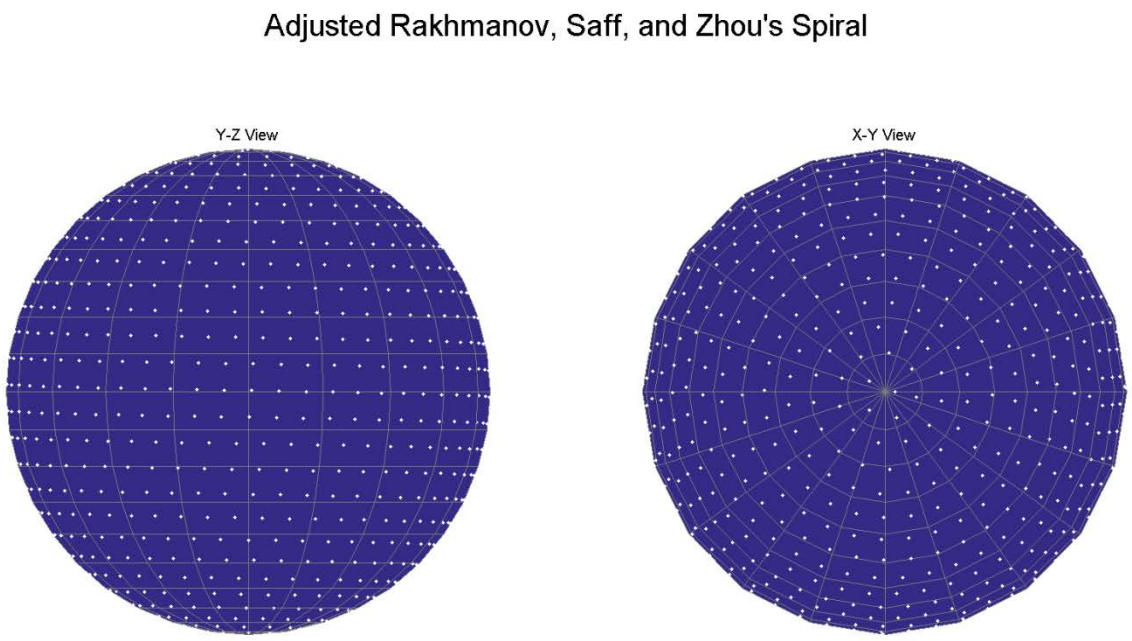

Fig. 29 One thousand points of adjusted Rakhmanov, Saff, and Zhou's spiral on the surface of a sphere

Is the resulting spiral an improvement? That would depend on the definition of what makes one distribution of points better (i.e., more evenly spaced) than the other. To compare the distribution of these adjusted RSZ spiral points to those of the original RSZ spiral method, we again have to first establish a metric. As in the 2-D analogue of evenly spaced points on a disc, we are going to calculate Voronoi diagrams, but this time we will be working on the surface of the sphere instead of within the plane. Our metric will then be the standard deviation of the surface area of the cells (i.e., of the solid angles).

Figures 30 and 31show Voronoi diagrams and solid angle standard deviation for both the original and adjusted RSZ spiral methods for 1,000 points. Although both methods produce distributions of points that appear to be fairly evenly spaced, the standard deviation of the solid angle of Voronoi cells of the adjusted RSZ spiral method is slightly more than 41% less than that of the original RSZ spiral method. This indicates that the adjusted RSZ spiral method produces a more evenly spaced set of points as measured by the stated metric.

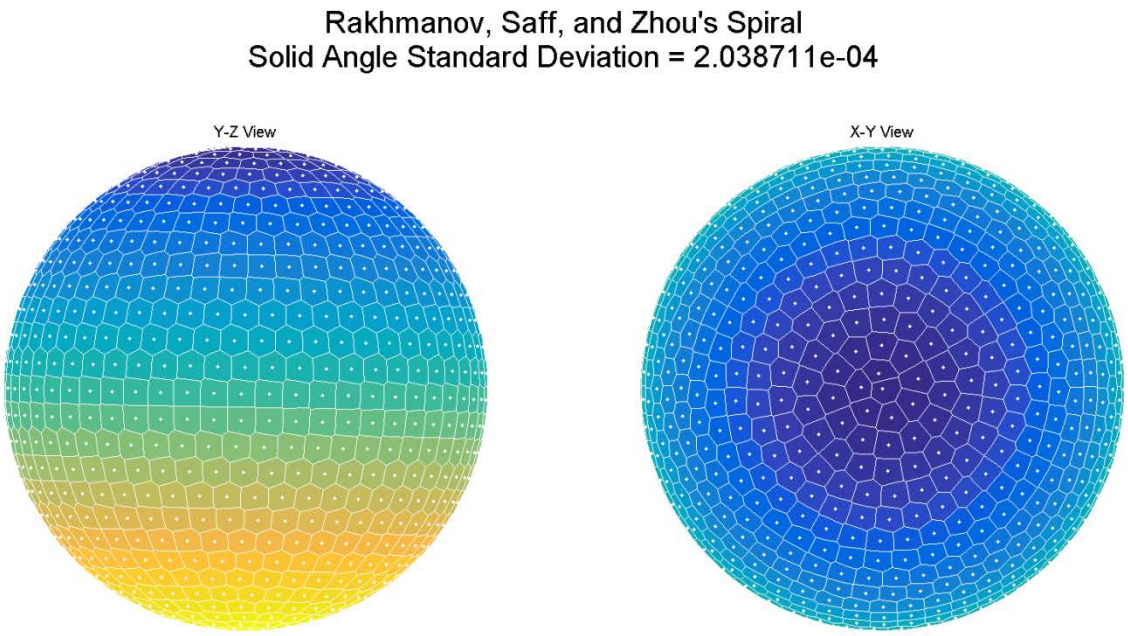

Fig. 30 Voronoi diagram of Rakhmanov, Saff, and Zhou's spiral on the surface of a sphere

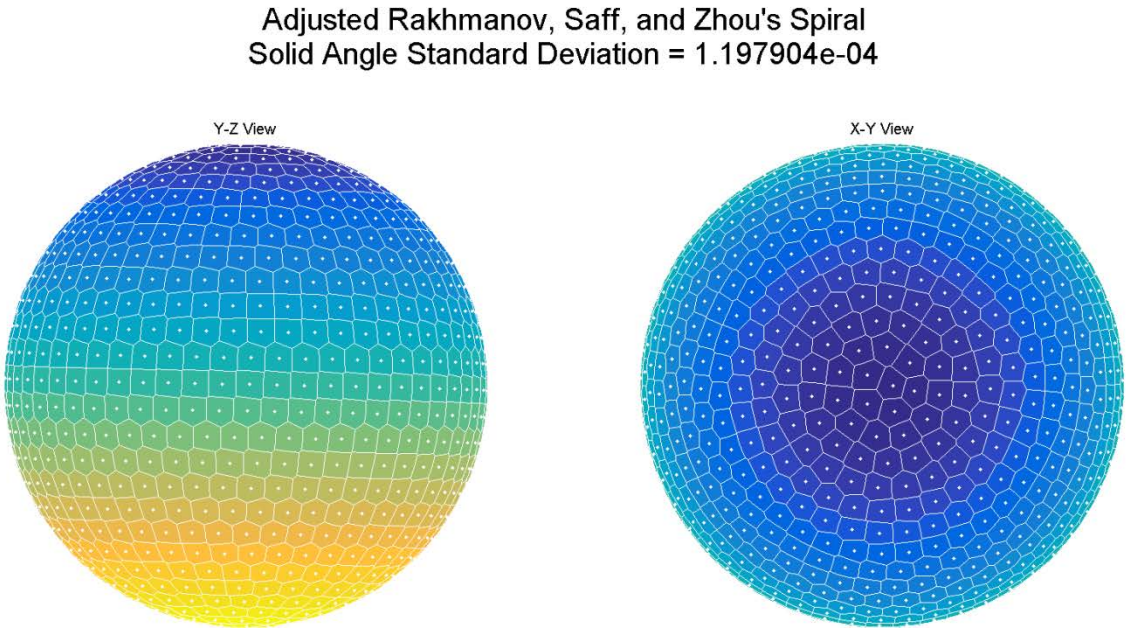

Fig. 31 Voronoi diagram of adjusted Rakhmanov, Saff, and Zhou's spiral on the surface of a sphere

Finally, taking a lesson from Vogel's method as stated in Section 5.3, we offer the second potential improvement to the RSZ spiral by changing the θ_k increment in Eq. 86 from Rakhmanov, Saff, and Zhou's value of $C/\sqrt{n}$, to the following:

$$\theta_k = k * \delta, \quad 0 \leq k \leq n-1, \tag{91}$$

where $\delta = \pi\left(3 - \sqrt{5}\right)$ is the golden angle as in Vogel's method. The other equations remain the same as those used in the adjusted RSZ spiral (Eqs. 82, 85, 89, and 90) and the spiral is re-spaced as shown in Fig. 32.

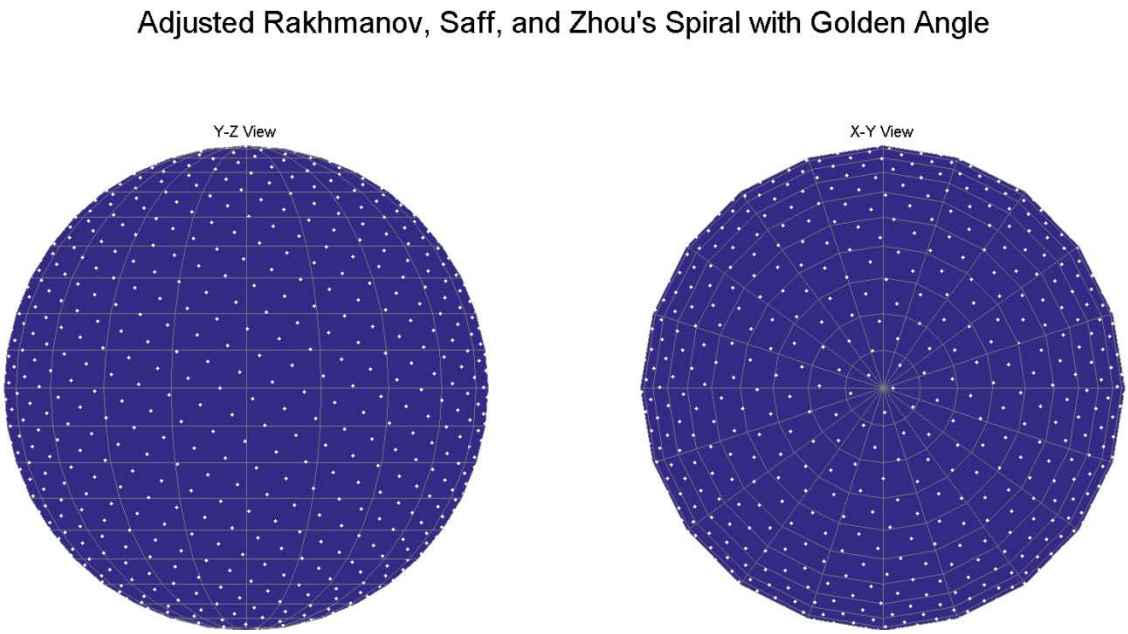

Fig. 32 One thousand points of adjusted Rakhmanov, Saff, and Zhou's spiral with the golden angle on the surface of a sphere

Figures 31 and 33 show Voronoi diagrams and solid angle standard deviation for both the adjusted RSZ spiral method and adjusted RSZ spiral method with golden angle for 1,000 points. Although both methods produce distributions of points that appear to be fairly evenly spaced, the standard deviation of the solid angle of Voronoi cells of the adjusted RSZ spiral method with golden angle is slightly more than 27% less than that of the adjusted RSZ spiral method. This indicates that the adjusted RSZ spiral method with golden angle produces a more evenly spaced set of points as measured by the stated metric.

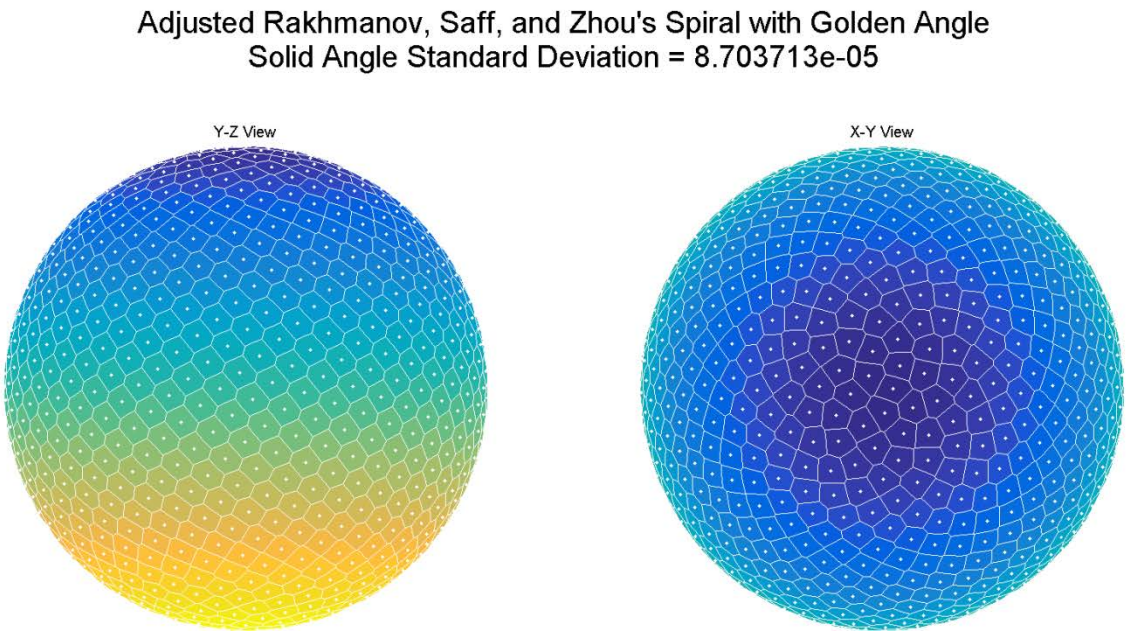

Fig. 33 Voronoi diagram of Rakhmanov, Saff, and Zhou's spiral with the golden angle on the surface of a sphere

6.3 Bauer

The final method to be presented is that of Bauer.[19] In 2000, Bauer presented a straightforward, nonrecursive spherical spiral for testing algorithms for stellar attitude determination analyses. Like Rakhmanov, Saff, and Zhou's spiral, Bauer's is an analytic spiral that is simple to implement. Bauer's spiral has the form

$$L = \sqrt{n\,\pi}, \tag{92}$$

$$z_k = 1 - \frac{2k-1}{n}, \qquad 1 \le k \le n, \tag{93}$$

$$\varphi_k = \cos^{-1}(z_k), \qquad 1 \le k \le n, \tag{94}$$

$$\theta_k = L\,\varphi_k, \qquad 1 \le k \le n, \tag{95}$$

$$x_k = \sin(\varphi_k)\,\cos(\theta_k), \quad 1 \le k \le n, \tag{96}$$

$$y_k = \sin(\varphi_k)\,\sin(\theta_k), \quad 1 \le k \le n. \tag{97}$$

Bauer's spiral with 1,000 points is shown in Fig. 34. Figure 35 shows the Voronoi diagram and solid angle standard deviation for the same set of points. Here we can see that the standard deviation of the solid angle of Voronoi cells of Bauer's spiral method is extremely close to (about 1% higher than) that of the adjusted RSZ spiral method with golden angle. This indicates that Bauer's method and the adjusted RSZ spiral method with golden angle produce equivalently evenly spaced point distributions as measured by the stated metric.

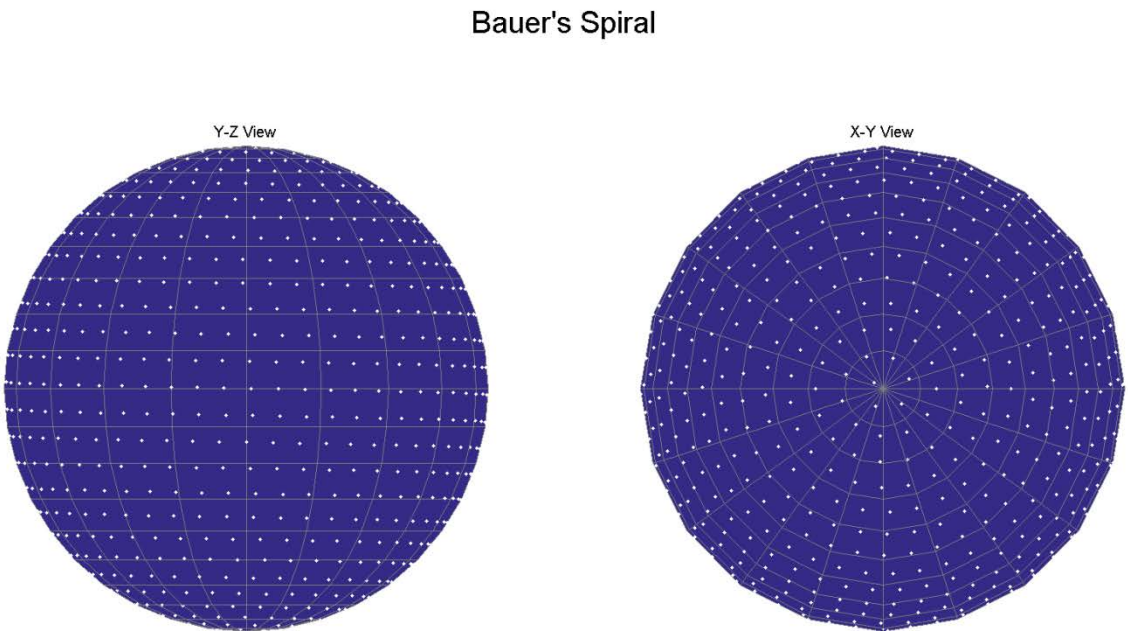

Fig. 34 One thousand points of Bauer's spiral on the surface of a sphere

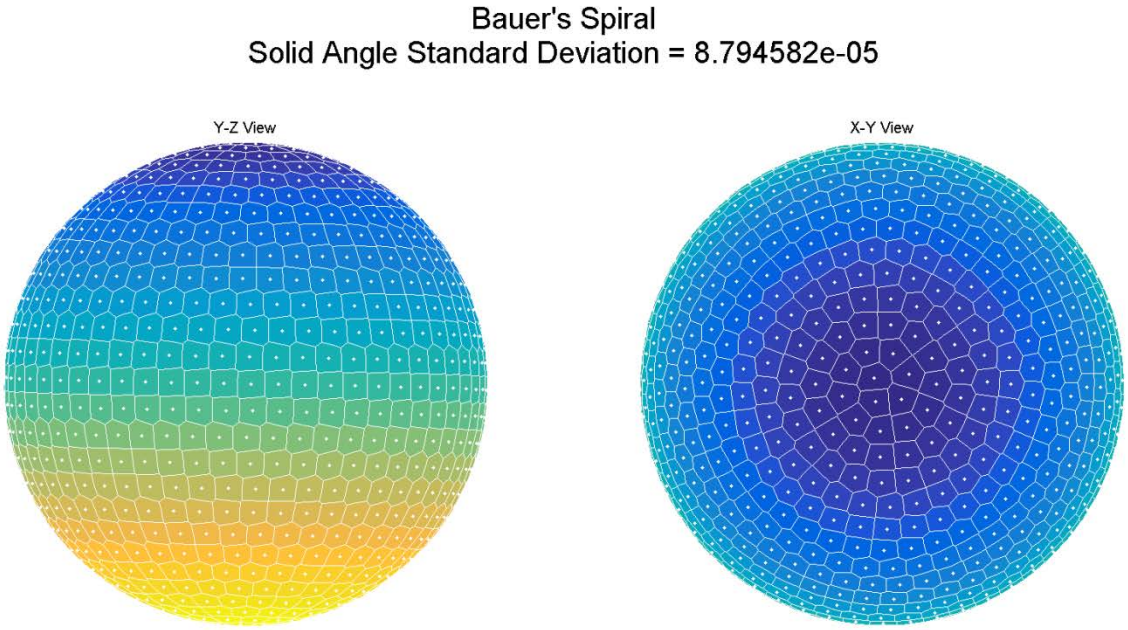

Fig. 35 Voronoi diagram of Bauer's spiral on the surface of a sphere

7. Conclusions

The algorithms presented in this report offer only a small glimpse into the complex and unsolved problem of point picking and distributing. They are the algorithms that have proved most useful for myself in a large variety of applications. Many of the algorithms are well known (e.g., any of the point picking algorithms) but not always well documented. In such cases, it was my aim not only to document, but also to offer some explanation or proof for why the algorithm is correct and why it works.

All but one of the point distributing algorithms presented are formally attributed to the person or people who discovered/derived them. While I do not claim to be the first person to derive what I have called the spiral method, I was not able to find such a method and/or equations via an extensive literature search which included both the internet and many scientific and mathematical journals and textbooks. I would be very interested to know whether or not such equations have been published elsewhere and welcome any such information and/or comments. Furthermore, I highly suggest that the interested reader read through the sources referenced in this report.

8. References and Notes

1. (U) Yager RJ, Patterson C. Modular-munition, dual-warhead concept analysis. Aberdeen Proving Ground (MD): Army Research Laboratory (US); 2013 July. Report No.: ARL-TR-6516, (SECRET).
2. (U) Strohm L, Arthur M. Modular lethality: examining changes in module placement for multi-target defeat. Aberdeen Proving Ground (MD): Army Research Laboratory (US); 2015 May. Report No.: ARL-TR-7246, (SECRET).
3. Strohm L. Modular lethality: methodology for resource allocation. Aberdeen Proving Ground (MD): Army Research Laboratory (US); in press.
4. Muller ME. Some continuous Monte Carlo methods for the Dirichlet problem. Ann Math Stat. 1956;27(3):569–589.
5. Muller ME. A note on a method for generating points uniformly on n-dimensional spheres. Communications of the ACM. 1959;2(4):19–20. Note: There is an error in the sign of the exponent in the equation for step 2 of Muller's Method in this reference.
6. Gautschi W. The spiral of Theodorus, numerical analysis, and special functions. Journal of Computational and Applied Mathematics. 2010;235(4):1042–1052.
7. Vogel H. A better way to construct the sunflower head. Mathematical Biosciences. 1978;44(3–4):178–189.
8. Vogel referred to the spiral as a cyclotron spiral, but the author was unable to find any other resources that refer to the spiral in question by this name.
9. Vogel's method is actually a single spiral method.
10. Thomson JJ. On the structure of the atom: an investigation of the stability and periods of oscillation of a number of corpuscles arranged at equal intervals around the circumference of a circle; with application of the results to the theory of atomic structure. Philosophical Magazine. 1904;7(39):237–265. Series 6.
11. Whyte LL. Unique arrangements of points on a sphere. The American Mathematical Monthly. 1952;59(9):606–611.
12. All points are equidistant from their nearest neighbors.
13. Proofs can be found in a variety of reference books. For one such proof, see section 4.1.2 of O-Rourke J. Computational Geometry in C. Cambridge (United Kingdom): Cambridge University Press; 1993.

14. Spaceship Earth. Walt Disney World; [accessed 2014 Nov 7] https://disneyworld.disney.go.com/attractions/epcot/spaceship-earth/.

15. Long Island Green Dome. [accessed 2014 Jul 7] https://www.facebook.com/ligreendome/map?activecategory=Photos&session_id=1334292191.

16. Environment Canada. Biosphere, environment museum. [accessed 2014 Nov 7] http://www.ec.gc.ca/biosphere/.

17. Missouri Botanical Garden. Climatron. [accessed 2014 Nov 7] http://www.missouribotanicalgarden.org/gardens-gardening/our-garden/gardens-conservatories/conservatories/climatron.aspx.

18. Rakhmanov EA, Saff EB, Zhou YM. Minimal discrete energy on the sphere. Mathematical Research Letters. 1994;1(6):647–662.

19. Bauer R. Distribution of points on a sphere with application to star catalogs. Journal of Guidance, Control, and Dynamics. 2000;23(1):130–137.

INTENTIONALLY LEFT BLANK

Appendix. Limit Evaluation from Section 5.1

This appendix appears in its original form, without editorial change.

Claim: $\lim_{n\to\infty}\lim_{k\to n} 2k+1-2\sqrt{k}\,\sqrt{k+1}\,\cos\left(\frac{\sqrt{k+1}-\sqrt{k}}{b}\right)=\frac{1}{4b^2}$.

Proof: Let $f(x)=2x+1-2\sqrt{x}\,\sqrt{x+1}\,\cos\left(\frac{\sqrt{x+1}-\sqrt{x}}{b}\right)$. Then

$$\lim_{x\to\infty} f(x)=\lim_{x\to\infty} 1+2x-2\sqrt{x(x+1)}\,\cos\left(\frac{\sqrt{x+1}-\sqrt{x}}{b}\right)$$

$$=\lim_{x\to\infty} 1+2x-2\sqrt{x(x+1)}\,\cos\left(\left(\frac{\sqrt{x+1}-\sqrt{x}}{b}\right)\left(\frac{\sqrt{x+1}+\sqrt{x}}{\sqrt{x+1}+\sqrt{x}}\right)\right)$$

$$=\lim_{x\to\infty} 1+2x-\,2\sqrt{x(x+1)}\,\cos\left(\frac{1}{b}\left(\frac{1+x-x}{\sqrt{x+1}+\sqrt{x}}\right)\right)$$

$$=\lim_{x\to\infty} 1+2x-2\sqrt{x(x+1)}\,\cos\left(\frac{1}{b}\left(\frac{1}{\sqrt{x+1}+\sqrt{x}}\right)\right).$$

Let $z=\frac{1}{x}$. Then

$$\lim_{x\to\infty} f(x)=\lim_{z\to 0} f\left(\frac{1}{z}\right)$$

$$=\lim_{z\to 0} 1+\frac{2}{z}-2\sqrt{\frac{1}{z}\left(\frac{1}{z}+1\right)}\,\cos\left(\frac{1}{b}\left(\frac{1}{\sqrt{\frac{1}{z}+1}+\sqrt{\frac{1}{z}}}\right)\right)$$

$$=\lim_{z\to 0} 1+\frac{2}{z}-2\sqrt{\frac{1}{z}\left(\frac{1}{z}+1\right)}\,\cos\left(\frac{1}{b}\left(\frac{1}{\sqrt{\frac{1+z}{z}}+\sqrt{\frac{1}{z}}}\right)\right)$$

$$=\lim_{z\to 0} 1+\frac{2}{z}-2\sqrt{\frac{1}{z}\left(\frac{1}{z}+1\right)}\,\cos\left(\frac{1}{b}\left(\frac{\sqrt{z}}{1+\sqrt{z+1}}\right)\right).$$

Let $g(z)=\sqrt{\frac{1}{z}\left(\frac{1}{z}+1\right)}$, and calculate the Laurent series about $z=0$.

$$g(z)=\sqrt{\frac{1}{z}\left(\frac{1}{z}+1\right)}=\sum_{n=-\infty}^{\infty} a_n z^n$$

where

$$a_n=\frac{1}{2\pi i}\oint_\gamma \frac{g(z)}{z^{n+1}}\,dz,$$

and the path of integration, γ, is counterclockwise around any closed, rectifiable path containing no self-intersections, and enclosing, but not containing, the point $z=0$.

Note that

$$a_n = \frac{1}{2\pi i}\oint_\gamma \frac{g(z)}{z^{n+1}}dz = \frac{1}{2\pi i}\oint_\gamma \frac{\sqrt{\frac{1}{z}\left(\frac{1}{z}+1\right)}}{z^{n+1}}dz = \frac{1}{2\pi i}\oint_\gamma \sqrt{\frac{1}{z^2}(1+z)}dz$$

$$= \frac{1}{2\pi i}\oint_\gamma \frac{1}{z^{n+2}}\sqrt{1+z}\,dz = \frac{1}{2\pi i}\oint_\gamma A(z)dz$$

where $A(z) = \frac{1}{z^{n+2}}\sqrt{1+z}$, and that $A(z)$ is analytic everywhere for $n \leq -2$.

Therefore, by the Cauchy integral theorem*

$$a_n = \frac{1}{2\pi i}\oint_\gamma A(z)dz = 0 \text{ for } n \leq -2.$$

So we need only to consider $n = -1, 0, 1, 2, \ldots$

$n = -1$:

$$a_{-1} = \frac{1}{2\pi i}\oint_\gamma \frac{1}{z}\sqrt{1+z}dz$$

$z = 0$ is a pole of order 1, therefore

$$a_{-1} = \frac{1}{2\pi i}\oint_\gamma \frac{1}{z}\sqrt{1+z}dz = Res_0\left(\frac{1}{z}\sqrt{1+z}\right) = \lim_{z\to 0}\left(z\left(\frac{1}{z}\sqrt{1+z}\right)\right) = 1.$$

$n = 0$:

$$a_0 = \frac{1}{2\pi i}\oint_\gamma \frac{1}{z^2}\sqrt{1+z}dz$$

$z = 0$ is a pole of order 2, therefore

$$a_0 = \frac{1}{2\pi i}\oint_\gamma \frac{1}{z^2}\sqrt{1+z}dz = Res_0\left(\frac{1}{z^2}\sqrt{1+z}\right) = \lim_{z\to 0}\frac{d}{dz}\left(z^2\left(\frac{1}{z^2}\sqrt{1+z}\right)\right)$$

$$= \lim_{z\to 0}\frac{1}{2}(1+z)^{-1/2} = \frac{1}{2}.$$

$n = 1$:

$$a_1 = \frac{1}{2\pi i}\oint_\gamma \frac{1}{z^3}\sqrt{1+z}dz$$

$z = 0$ is a pole of order 3, therefore

$$a_1 = \frac{1}{2\pi i}\oint_\gamma \frac{1}{z^3}\sqrt{1+z}dz = Res_0\left(\frac{1}{z^3}\sqrt{1+z}\right)$$

$$= \frac{1}{2}\lim_{z\to 0}\frac{d^2}{dz^2}\left(z^3\left(\frac{1}{z^3}\sqrt{1+z}\right)\right) = \frac{1}{2}\lim_{z\to 0} -\frac{1}{4}(1+z)^{-3/2} = -\frac{1}{8}.$$

* Also know as the Cauchy-Goursat theorem: Let $D \subseteq \mathbb{C}$, D open and simply connected, let $f: D \to \mathbb{C}$ be a holomorphic (analytic) function, and let γ be a rectifiable path in D whos start point is equal to its end point. Then $\oint_\gamma f(z)dz = 0$.

Therefore

$$g(z) = \sqrt{\frac{1}{z}\left(\frac{1}{z}+1\right)} = \sum_{n=-\infty}^{\infty} a_n z^n = \frac{1}{z} + \frac{1}{2} - \frac{z}{8} + O(z^2).$$

Now let $h(z) = \cos\left(\frac{1}{b}\left(\frac{\sqrt{z}}{1+\sqrt{z+1}}\right)\right)$, and since $h(z)$ is differentiable at $z = 0$, the Maclaurin series of $h(z)$ is given by

$$h(z) = h(0) + h'(0)z + O(z^2).$$

Therefore,

$$h'(z) = \left(\frac{\sqrt{z}}{2b\sqrt{z+1}\left(1+\sqrt{z+1}\right)^2} - \frac{1}{2b\sqrt{z}\left(1+\sqrt{z+1}\right)}\right)\sin\left(\frac{1}{b}\left(\frac{\sqrt{z}}{1+\sqrt{z+1}}\right)\right).$$

So let $h'(z) = h_1(z) - h_2(z)$ where

$$h_1(z) = \left(\frac{\sqrt{z}}{2b\sqrt{z+1}\left(1+\sqrt{z+1}\right)^2}\right)\sin\left(\frac{1}{b}\left(\frac{\sqrt{z}}{1+\sqrt{z+1}}\right)\right)$$

and $$h_2(z) = \left(\frac{1}{2b\sqrt{z}\left(1+\sqrt{z+1}\right)}\right)\sin\left(\frac{1}{b}\left(\frac{\sqrt{z}}{1+\sqrt{z+1}}\right)\right).$$

$h_2(z)$ is not defined at $z = 0$, but taking the limit as $z \to 0$ yields

$$\lim_{z\to 0} h_2(z) = \lim_{z\to 0}\left(\frac{1}{2b\sqrt{z}\left(1+\sqrt{z+1}\right)}\right)\sin\left(\frac{1}{b}\left(\frac{\sqrt{z}}{1+\sqrt{z+1}}\right)\right)$$

$$= \lim_{z\to 0}\frac{\sin\left(\frac{1}{b}\left(\frac{\sqrt{z}}{1+\sqrt{z+1}}\right)\right)}{2b\sqrt{z}\left(1+\sqrt{z+1}\right)}$$

$$= \frac{\lim_{z\to 0}\sin\left(\frac{1}{b}\left(\frac{\sqrt{z}}{1+\sqrt{z+1}}\right)\right)}{\lim_{z\to 0} 2b\sqrt{z}\left(1+\sqrt{z+1}\right)} = \frac{0}{0},$$

and applying L'Hospital's rule yields

$$\lim_{z\to 0} h_2(z) = \lim_{z\to 0}\frac{\frac{d}{dz}\left(\sin\left(\frac{1}{b}\left(\frac{\sqrt{z}}{1+\sqrt{z+1}}\right)\right)\right)}{\frac{d}{dz}\left(2b\sqrt{z}\left(1+\sqrt{z+1}\right)\right)}$$

$$= \lim_{z\to 0}\frac{\cos\left(\frac{1}{b}\left(\frac{\sqrt{z}}{1+\sqrt{z+1}}\right)\right)}{b\left(1+\sqrt{z+1}\right)\left(1+2z+\sqrt{z+1}\right)} = \frac{1}{8b^2}.$$

So the singularity of $h_2(z)$ at $z = 0$ can be removed, and $h_2(z)$ becomes

$$h_2(z) = \begin{cases} \frac{1}{8b^2}, & z = 0 \\ \left(\frac{1}{2b\sqrt{z}\left(1+\sqrt{z+1}\right)}\right)\sin\left(\frac{1}{b}\left(\frac{\sqrt{z}}{1+\sqrt{z+1}}\right)\right), & otherwise \end{cases}.$$

Therefore

$$h'(z) = h_1(z) - h_2(z)$$

$$\Longrightarrow h'(0) = h_1(0) - h_2(0) = 0 - \frac{1}{8b^2}$$

$$\Longrightarrow h(z) = \cos\left(\frac{1}{b}\left(\frac{\sqrt{z}}{1+\sqrt{z+1}}\right)\right) = h(0) + h'(0)z + O(z^2) = 1 - \frac{z}{8b^2} + O(z^2).$$

Finally, $g(z) = \sqrt{\frac{1}{z}\left(\frac{1}{z}+1\right)} = \frac{1}{z} + \frac{1}{2} - \frac{z}{8} + O(z^2)$

and $h(z) = \cos\left(\frac{1}{b}\left(\frac{\sqrt{z}}{1+\sqrt{z+1}}\right)\right) = 1 - \frac{z}{8b^2} + O(z^2)$

imply that $\lim_{x\to\infty} f(x) = \lim_{z\to 0} f\left(\frac{1}{z}\right)$

$$= \lim_{z\to 0} 1 + \frac{2}{z} - 2\sqrt{\frac{1}{z}\left(\frac{1}{z}+1\right)}\cos\left(\frac{1}{b}\left(\frac{\sqrt{z}}{1+\sqrt{z+1}}\right)\right)$$

$$= \lim_{z\to 0} 1 + \frac{2}{z} - 2\, g(z)\, h(z)$$

$$= \lim_{z\to 0} 1 + \frac{2}{z} - 2\left(\frac{1}{z} + \frac{1}{2} - \frac{z}{8} + O(z^2)\right)\left(1 - \frac{z}{8b^2} + O(z^2)\right)$$

$$= \lim_{z\to 0} 1 + \frac{2}{z} - 2\left(\frac{1}{z} + \frac{1}{2} - \frac{1}{8b^2} + O(z)\right)$$

$$= \lim_{z\to 0} 1 + \frac{2}{z} - \frac{2}{z} - 1 + \frac{1}{4b^2} + O(z) = \frac{1}{4b^2}.$$

■

1 DEFENSE TECHNICAL
(PDF) INFORMATION CTR
DTIC OCA

2 DIRECTOR
(PDF) US ARMY RESEARCH LAB
RDRL CIO LL
IMAL HRA MAIL & RECORDS MGMT

1 GOVT PRINTG OFC
(PDF) A MALHOTRA

1 DIR USARL
(PDF) RDRL WML A
M ARTHUR